The *Drosophila l(1)zw10* Gene Product, Required for Accurate Mitotic Chromosome Segregation, Is Redistributed at Anaphase Onset

Byron C. Williams,* Tim L. Karr,‡ John M. Montgomery,* and Michael L. Goldberg*

*Section of Genetics and Development, Biotechnology Building, Cornell University, Ithaca, New York 14853-2703; and
‡Department of Biochemistry and the Beckman Institute, University of Illinois, Urbana, Illinois 61801

Abstract. Mutations in the gene *l(1)zw10* disrupt the accuracy of chromosome segregation in a variety of cell types during the course of *Drosophila* development. Cytological analysis of mutant larval brain neuroblasts shows very high levels of aneuploid cells. Many anaphase figures are aberrant, the most frequent abnormality being the presence of lagging chromosomes that remain in the vicinity of the metaphase plate when the other chromosomes have migrated toward the spindle poles. Finally, the centromeric connection between sister chromatids in mutant neuroblasts treated with colchicine often appears to be broken, in contrast with similarly treated control neuroblasts. The 85-kD protein encoded by the *l(1)zw10* locus displays a dynamic pattern of localization in the course of the embryonic cell cycle. It is excluded from the nuclei during interphase, but migrates into the nuclear zone during prometaphase. At metaphase, the *zw10* antigen is found in a novel filamentous structure that may be specifically associated with kinetochore microtubules. Upon anaphase onset, there is an extremely rapid redistribution of the *zw10* protein to a location at or near the kinetochores of the separating chromosomes.

ONE strategy to define the molecular components of structures required for accurate chromosome segregation during mitosis is the study of mutations that disrupt this process. This approach has the advantage that it may illuminate important molecules present only in modest concentrations; moreover, the mutant phenotypes may yield useful clues to the function of the corresponding gene products. Several techniques have been developed for the identification of mutations in *Drosophila melanogaster* that disrupt mitotic chromosome behavior (reviewed in Gatti and Goldberg, 1991). Extensive screening for such mitotic mutants has thus far revealed mutations in only two loci that cause a high percentage of dividing cells to become aneuploid. These genes are *rough deal* (*rod*) and *lethal on the X chromosome zeste-white 10* (*l[1]zw10*, subsequently abbreviated here as *zw10*; also known as *mit[1]115* [Lindsley and Zimm, 1990]) (Smith et al., 1985; Karess and Glover, 1989; Gatti and Baker, 1989).

In this paper, we report both a detailed analysis of the cytological phenotypes caused by lesions in *zw10*, as well as molecular studies on the *zw10* locus and the protein it encodes. Our results reveal a requirement for *zw10* function at a time near anaphase onset for the accuracy of sister chromatid disjunction and/or early anaphase chromatid movement. Such a role for the *zw10* product appears to be reflected in the remarkable series of transformations in the intracellular location of this protein we have observed during the cell cycle.

Materials and Methods

Drosophila Stocks

The *zw10* alleles $zw10^{S1}$, a spontaneous mutation (Schalet, 1986), and $zw10^{S2M}$, a mutation generated in a *mei-9* background (Lindsley and Zimm, 1990), were obtained from A. Schalet (Yale University, New Haven, CT). B. Judd (National Institute of Environmental Health Sciences, Research Triangle Park, NC) kindly provided two additional *zw10* alleles ($zw10^{65i20}$, induced by ethyleneimine; and $zw10^{65i21}$, induced by ethyleneimine and x rays), representative alleles of nearby lethal complementation groups ($zw4^{63e4}$, $zw13^{e50}$, and $zw2^{62b11}$), and the rearrangements $Df(1)w^{rJ1}$, *Df(1)64j4*, and $Dp(1;2)w^{+70h31}$. These strains have been described in detail by Judd et al. (1972). The allele $zw10^{ts}$ (Smith et al., 1985) was received from B. Baker (Stanford University, Palo Alto, CA). Mutations and rearrangements were maintained in females over either of the X chromosome balancers *FM7a* or *FM6*, *169a*, or in males covered by the Y chromosome derivatives w^+Y or $B^sw^+y^+Y$ (see Lindsley and Zimm, 1986, 1987, 1990 for further explanation of chromosomes and genetic symbols used).

To obtain larvae hemizygous for mutant *zw10* alleles ($zw10^x$), males of genotype $zw10^x/w^+Y$ were crossed with $C(1)DX,y\,f/Y;ry^{506}$ females (from D. Glover, Dundee University, UK). Male larvae, distinguished by the external morphology of the larval gonad, are thus $zw10^x/Y$. Females heterozygous for *zw10* mutations and deletions of the *zw10* region were generated by crossing $zw10^x/FM7a$ females to $Df(1)w^{rJ1}/B^sw^+y^+Y$ males. Offspring larvae of interest ($zw10^x/Df(1)w^{rJ1}$) could be differentiated from their siblings by sex and by virtue of their yellow-colored (w^+) Malphigian tubules.

Stocks used in germline transformation experiments and subsequent genetic manipulations are described below.

Cytology

Metaphase figures were examined using standard cytological procedures

(Gatti et al., 1974; Gatti and Goldberg, 1991). Ganglia from wandering third instar larvae were dissected in 0.7% NaCl, incubated in 0.5 × 10^{-5} M colchicine in 0.7% NaCl for 1 h at 25°C, and then immersed in 0.5 M sodium citrate (hypotonic solution) for 7 min. The ganglia were then fixed for ~30 s in acetic acid/methanol/distilled water (11:11:2). Fixed brains were immediately transferred into a drop of aceto-orcein stain (2% orcein in 45% acetic acid) on a coverslip and squashed onto a glass slide. For examination of anaphases, the colchicine and hypotonic treatments were excluded from the above procedure. Cytological preparations according to a different protocol (González et al., 1988; Karess and Glover, 1989) yielded identical results (data not shown). Mitotic index was determined by averaging the number of cells undergoing mitosis per optic field under standardized conditions, using a phase-contrast Neofluar 100× oil-immersion Zeiss objective (Carl Zeiss, Inc., Thornwood, NY), 10× oculars, and the Optivar set at 1.25×.

Nucleic Acids

The preparation of recombinant DNA from plasmid, cosmid, or bacteriophage lambda vectors, or genomic DNA from *Drosophila* adults, has previously been noted (Gunaratne et al., 1986; Mansukhani et al., 1988*a*,*b*). Genomic clones were isolated either from an EMBL4 genomic library (Gunaratne et al., 1986), or from a cosmid library kindly provided by J. Tamkun (University of Colorado, Boulder, CO). Restriction fragments were subcloned into the polylinker of Bluescript KS$^+$ (Stratagene Inc., La Jolla, CA). Transfer of DNA from agarose gels to Gene Screen Plus membranes (New England Nuclear, Boston, MA) was carried out using the alkaline blot method (Sambrook et al., 1989). For radiolabeling, primer extensions from either purified DNA or DNA fragments excised from low-melt agarose gels (SeaPlaque, FMC Marine Colloids, Rockland, ME) were performed essentially as described by Feinberg and Vogelstein (1983). In situ hybridization of DNA fragments labeled with biotin-11-dUTP to salivary gland polytene chromosomes was performed as previously described (Gunaratne et al., 1986) using the Detek kit (Enzo Biochemistry Inc., New York, NY).

Poly(A)+ RNA was isolated from staged wild-type *Drosophila* according to the procedure of Dombrádi et al. (1989). Electrophoresis of glyoxalated poly(A)+ RNA on agarose gels, transfer to Hybond-N membranes, and hybridization of Northern blots with labeled probes was also carried out as detailed by the same authors.

Full length *zwl0* cDNA clones were isolated from a *Drosophila* imaginal disc cDNA library supplied by Dr. Nicholas Brown (Harvard University, Cambridge, MA). Since the pNB40 vector used allows directional cDNA cloning (Brown and Kafatos, 1988), the orientation of transcription could be readily determined by restriction analysis. A *Bgl*II-*Not*I fragment containing the entire *zwl0* cDNA was cloned into the *Bam*HI and *Not*I sites of Bluescript KS−, yielding the construct 20.4KS−. Deletions were constructed using partial ExoIII nuclease digestion as described by Henikoff (1984) using the Erase-a-Base kit (Promega Corp., Madison, WI). 20.4KS− was digested with *Kpn*I and *Cla*I for deletions starting from the 5′-end of the cDNA, while *Sac*I and *Not*I were used for deletions starting from the 3′-end. Double stranded plasmid DNA was sequenced by the dideoxy chain termination method of Sanger et al. (1977) using the T7 DNA polymerase Sequenase (United States Biochemical Corp., Cleveland, OH), ^{35}S-dATP (Amersham Corp., Arlington Heights, IL), and gradient gels with wedge spacers (Bethesda Research Laboratories, Gaithersburg, MD). Both strands were sequenced completely and in duplicate, using standard Bluescript primers (Stratagene Inc.). To confirm the absence of introns around the site of the *zwl0^{S1}* insertion, primers derived from the *zwl0* cDNA sequence were synthesized and used for sequencing the wild-type genomic clone. Sequence analysis was carried out using the GCG package, and FASTA searches of Genbank, EMBL, PIR, Swiss-Prot, and NBRF databanks (Devereux et al., 1984).

Germline Transformation

A 4.6 kb *Bam*HI fragment from the cosmid genomic clone cosB was inserted into the *Bam*HI site of pW8, a transformation vector carrying a mini-*white*$^+$ gene (Klemenz et al., 1987). The resulting construct was injected into *w; Sb e Delta2-3/TM6, Ubx* embryos, which express transposase (Robertson et al., 1988); G0 survivors were single-pair mated to z^1w^{11e4} and the G1 was screened for pigmented eye color. Independently derived transformants were isolated and mated to z^1w^{11e4} to determine the linkage of w^+ and to maintain the line. In one line (1-1) the fragment had integrated into the *Delta2-3, Sb* chromosome and was subsequently crossed away from *Delta2-3* and *Sb*. In two others (2A and 3A), w^+ was linked to *Ubx*, a marker on *TM6*. Males containing these autosomally located transduced DNA fragments were mated with *zwl0^x*/Balancer females to test for the presence of non-*Bar* eyed *zwl0^x* male progeny in the next generation. Three different *zwl0* alleles (*zwl0^{S1}*, *zwl0^{S2M}*, and *zwl0^{65i20}*) were rescued by the 1-1, 2A and 3A transformant lines. In each case, the low viability, sterility, eye morphology, and mitotic (cytological) phenotypes of the *zwl0* mutations were complemented by the autosomal fragment.

Antibody Production and Purification

A 2.2-kb *Nru*I-*Not*I fragment from the full length *zwl0* cDNA was blunt-end ligated in frame with the *lacZ* gene in pWR590-2 (Guo et al., 1984). An overnight culture of the XLI-Blue bacterial strain (Stratagene Inc.) carrying the *lacZ-zwl0* fusion clone was grown, induced with isopropylthio-β-D-galactoside (IPTG), harvested, and analyzed by previously described methods (Mansukhani et al., 1988*a*,*b*). The gel was stained with 50% methanol containing Coomassie brilliant blue for 5 min, then destained with distilled water. The fusion protein band was excised, placed in a dialysis bag, and electroeluted for 4 h at 100 V. Protein was dialyzed in several changes of PBS (formulation of Karr and Alberts, 1986) and the concentration checked by SDS-PAGE. To verify the identification of the fusion protein, Western blotting was used as previously described (Mansukhani et al., 1988*b*), except that alkaline phosphatase-conjugated anti-rabbit IgG (Sigma Chemical Co., St. Louis, MO) was used in the detection system (Sambrook et al., 1989). Fusion protein was injected into two rabbits and boosted twice thereafter. Both preimmune and immune sera were collected separately for each rabbit.

To facilitate purification of anti-*zwl0* antibodies, and to exclude antibodies reacting exclusively to the β-galactosidase moiety of the *lacZ-zwl0* fusion described above, a *trpE-zwl0* fusion was constructed in the vector pATH3 (Dieckmann and Tzagoloff, 1985). The same *zwl0* cDNA *Nru*I-*Not*I fragment used to make *lacZ-zwl0* was blunt-end ligated into the *Bam*HI site of pATH3 (which was made blunt by filling in with Klenow DNA polymerase), so that *zwl0* was in frame with *trpE* sequences. The resulting construct was called *pATH3-zwl0*. Derivatives containing shorter *zwl0*-specific segments were created by digesting *pATH3-zwl0* with *Xho*I or *Hind*III and recircularizing the products in a very dilute ligation mixture. The *Xho*I derivative (*trpE-zwl0X*) lacks the central portion of *zwl0* (amino acids 177–495) and the *Hind*III derivative (*trpE-zwl0H*) does not contain the COOH-terminal end (amino acids 528–721). It should be noted that all *lacZ-zwl0* and *trpE-zwl0* fusion proteins lack the NH_2 terminus of the *zwl0* protein (amino acids 1–76).

trpE-zwl0 fusion proteins were induced as described by Dieckmann and Tzagoloff (1985). Induced *trpE-zwl0* fusion proteins were isolated as the insoluble fraction after the lysis of cells with lysozyme and NP-40 in TEN buffer (50 mM Tris·HCl, pH 7.5, 0.5 mM EDTA, 0.3 M NaCl). Protein was solubilized in cracking buffer (0.01 M sodium phosphate, pH 7.2, 1% 2-mercaptoethanol, 1% SDS, 8 M urea) and dialyzed overnight in PBS.

For immunoaffinity purification, the *trpE-zwl0* fusion protein of interest was coupled to washed cyanogen bromide-activated Sepharose 4B (Sigma Chemical Co.) for 16 h in coupling buffer (0.1 M $NaHCO_3$, pH 8.3, 0.5 M NaCl) at 4°C. The buffer was removed and the remaining active groups blocked for 1 h at room temperature in 0.2 M glycine, pH 8.0. The fusion protein-coupled resin was poured into a column and washed extensively with PBS. Crude serum diluted 1:10 in PBS was first applied to a column of Sepharose 4B–coupled insoluble protein extract from XLI Blue cells not expressing the fusion protein and prepared according to the same protocol. The resultant preadsorbed crude serum was then recirculated during a period of 12 h through the column containing the immobilized fusion protein. The column was washed extensively with PBS, and the bound antibody was eluted with 0.2 M glycine, pH 2.7. The purified antibody solution (~100 μg/ml) was immediately neutralized by the addition of 1/7 vol. of 1 M Tris·HCl, pH 8.9, and dialyzed for 24 h in three changes of PBS.

This procedure was carried out separately for preimmune sera and immune sera obtained from each rabbit; results obtained with both rabbits were qualitatively identical. The preimmune sera failed to identify *zwl0* fusion proteins on Western blots, and did not detect signals above background in immunofluorescence experiments. Antibodies purified against the derivatives *trpE-zwl0X* and *trpE-zwl0H* generated identical results on Western blots and in embryo staining.

Immunofluorescence

Wild-type Oregon R embryos were collected for 2 h to enrich for the presence of syncytial blastoderm embryos. Embryos were washed, dechorionated, and fixed with formaldehyde in the presence of taxol as described

(Karr and Alberts, 1986). Alternatively, embryos were fixed directly in methanol-EGTA (Warn and Warn, 1986). Both procedures gave similar results upon staining embryos with the purified antibody, although the former method yielded a higher signal-background ratio.

Embryos were incubated in immunoaffinity purified anti-*zw10* antibody appropriately diluted in TBS + Triton (TBST)[1] (50 mM Tris·HCl, pH 7.4, 50 mM NaCl, 0.02% sodium azide, 0.1% Triton X-100) overnight at 4°C. The primary antibody was washed off in 4 × 5 min washes in TBST. Biotinylated goat anti-rabbit IgG (Vector Laboratories, Inc., Burlingame, CA) was added at 1/200 dilution (to a final concentration of 7.5 μg/ml) for 1–2 h at room temperature, after which the embryos were washed with TBST as before. Next, either streptavidin-rhodamine isothiocyanate (Jackson Immunoresearch Laboratories, Inc., West Grove, PA) or cell sorter grade avidin DS-rhodamine (Vector Laboratories, Inc.; final concentration 20 μg/ml) were added and incubated for 1 h at room temperature. The embryos were washed and Hoechst 33258 (Sigma Chemical Co.) was added to a final concentration of 0.05 μg/ml for 5 min. Finally, the embryos were washed briefly in TBST and mounted in glycerol containing n-propyl gallate or p-phenylenediamine. Identical results were obtained using, as the secondary antibody, rhodamine-conjugated goat anti-rabbit IgG from several sources (Sigma Chemical Co.; Boehringer Mannheim Corp., Indianapolis, IN; Jackson Immunoresearch Laboratories, Inc.). In all cases, staining with the above reagents carried out in the absence of the anti-*zw10* antibody or with purified preimmune sera did not identify any specific structures. Embryos were observed under epifluorescence using a Zeiss Axioskop (Carl Zeiss, Inc.) with a Neofluar 100× objective. Images were recorded with Kodak Technical Pan Film (Eastman Kodak Co., Rochester, NY).

Confocal microscopy was carried out using a Zeiss Axiovert 10 attached to a Bio-Rad MRC600 confocal imaging system (Bio-Rad Laboratories, Cambridge, MA) at Cornell, and a confocal imaging system (Carl Zeiss, Inc.) at the Beckman Institute. To view DNA with the confocal microscope, stained embryos were incubated overnight with chromomycin C (Sigma Chemical Co.). For visualization of MTs, mouse anti-tubulin antibody (from K. Kemphues, Cornell University, Ithaca, NY) was used followed by FITC-conjugated goat-anti-mouse IgG antibody (Sigma Chemical Co.) in the above procedure. BX63, a mouse mAb described by Frasch et al. (1986), was the gift of D. Glover, and was used to stain centrosomes.

Detecting zw10 on Western Blots

zw10/Y mutant larva (see above) were collected, dissected, and frozen in liquid nitrogen. Larval ganglia, embryos, larva, or adult flies were homogenized in Sample Buffer (62.5 mM Tris-HCl, pH 6.8; 5% 2-mercaptoethanol, 3% SDS, 10% glycerol, 0.1% bromophenol blue), immediately boiled for 5 minutes, then cooled on ice for 5 minutes, and pelleted. Supernatant protein was separated by SDS-PAGE. Western blotting was performed as described above for fusion proteins. Alternatively, the enhanced chemiluminescence (ECL) Western Blotting System (Amersham Corp.) was used essentially as described in the instruction manual. Briefly, anti-*zw10* crude serum was diluted 1/700 in 5% dried milk in Tween Tris Buffered Saline (TTBS; 20 mM Tris·HCl, 137 mM NaCl, 0.05% Tween-20, pH 7.6, shaking overnight at room temperature. After three 10-min washes in TTBS, the blot was incubated for 1 h in peroxidase-conjugated donkey anti-rabbit IgG (Amersham NA.934; Amersham Corp.) diluted 1/2,000 in milk-TTBS. After three 10-min washes in TTBS, the blots were processed for luminescence exactly as described in the instruction manual.

For subsequent incubation with other antibodies to confirm protein levels, the blots were washed in TTBS for 30 min at room temperature, and the same procedures followed as above.

Transfection

To overexpress the *zw10* protein in *Drosophila* Schneider line 2 (S2) tissue culture cells, the entire *zw10* cDNA, containing the first methionine as well as untranslated leader sequences, was cloned into the *Bam*HI site of pPAC, which contains the strong actin5C promoter (a gift of Mark Krasnow, Stanford University, Palo Alto, CA) to make the construct *pPAC-zw10*. S2 cells were grown in appropriate cell media (Gibco Laboratories, Grand Island, NY) plus FCS (Sigma Chemical Co.) for 1 d. *pPAC-zw10* DNA was transfected into the cells with the calcium-phosphate method (Xiao and Lis, 1989), then allowed to grow for 3 d. Cells were harvested by centrifugation and boiled in sample buffer as above.

1. *Abbreviations used in this paper*: KMT, kinetochore microtubule; MT, microtubule; PSCS, precocious sister chromatid separation; TBST, TBS + Triton; TTBS, Tween TBS.

Results

Cytological Characterization of Mutant Larval Brains

The viability of flies homozygous or hemizygous for mutant alleles of *zw10* is severely reduced. The majority of *zw10* mutant animals die during late larval and pupal stages (Shannon et al., 1972); survival through embryonic and early larval stages is thought to be ensured by maternal wild-type gene product from heterozygous mothers (Gatti and Baker, 1989; see also Discussion below). Division of brain neuroblasts and imaginal disk cells occurs during the third larval instar, and is required for subsequent adult metamorphosis but not for larval life itself. The third instar larvae of mitotic mutants thus contain populations of cells undergoing improper mitosis. In particular, the dividing cells in the neural ganglia (brain neuroblasts) of third instar larvae are well suited to cytological observation which may suggest the origin of the mitotic defect. To elucidate the role played by the *zw10* product in ensuring proper chromosome segregation during cell division, we have continued the analysis of mitosis in *zw10* mutant larval neuroblasts initiated by Smith et al. (1985).

Aneuploidy. In preparations of wild-type larval ganglia, four pairs of chromosomes are clearly visible in each metaphase figure (Fig. 1 *a*). However, a high proportion (~50%) of brain cells in animals homozygous or hemizygous for a variety of *zw10* alleles are hyperploid (Table I; Smith et al., 1985). This is almost certainly an underestimate of the number of cells with abnormal chromosome complements: because chromosomes may be lost during squashing, hypoploid nuclei have not been scored in these studies. Examples of hyperploid mitotic figures are shown in Fig. 1, *b* and *c*. The distribution of karyotypes (Table I) suggests that *zw10* mutations cause essentially random mitotic segregation of chromosomes, with all major chromosomes affected to a similar extent.

Abnormal Anaphases. Aneuploidy caused by *zw10* mutations clearly involves improper chromosome segregation at anaphase. In wild-type male larval ganglia, most anaphases resemble that shown in Fig. 1 *d*; only a small percentage of anaphases can be classified as aberrant. Conversely, a high frequency (~40%) of abnormal anaphases are present in neuroblasts of animals hemizygous for any of several *zw10* mutant alleles (Table II). The defect most often observed is the presence of one or more chromatids lagging at the metaphase plate when the remainder have already migrated to their respective poles (Fig. 1, *e* and *f*). In some cases, some chromatids are clearly pulled at their kinetochore but are nonetheless delayed in their approach to a pole, while other chromatids appear not to be subjected to poleward forces at the time of fixation (Fig. 1 *g*). It is of interest that lagging chromatids are often found in the near vicinity of their sisters, which thus appear to be similarly affected (Fig. 1, *f* and *g*). In a fraction of cases, anaphases are either completely disorganized (Fig. 1 *i*), or result in obviously unequal chromosome complements at the two spindle poles (Fig. 1 *h*). Any of these aberrant events at anaphase could potentially produce aneuploidy in daughter cells.

Precocious Sister Chromatid Separation. Smith et al. (1985) have suggested an alternative explanation for the high

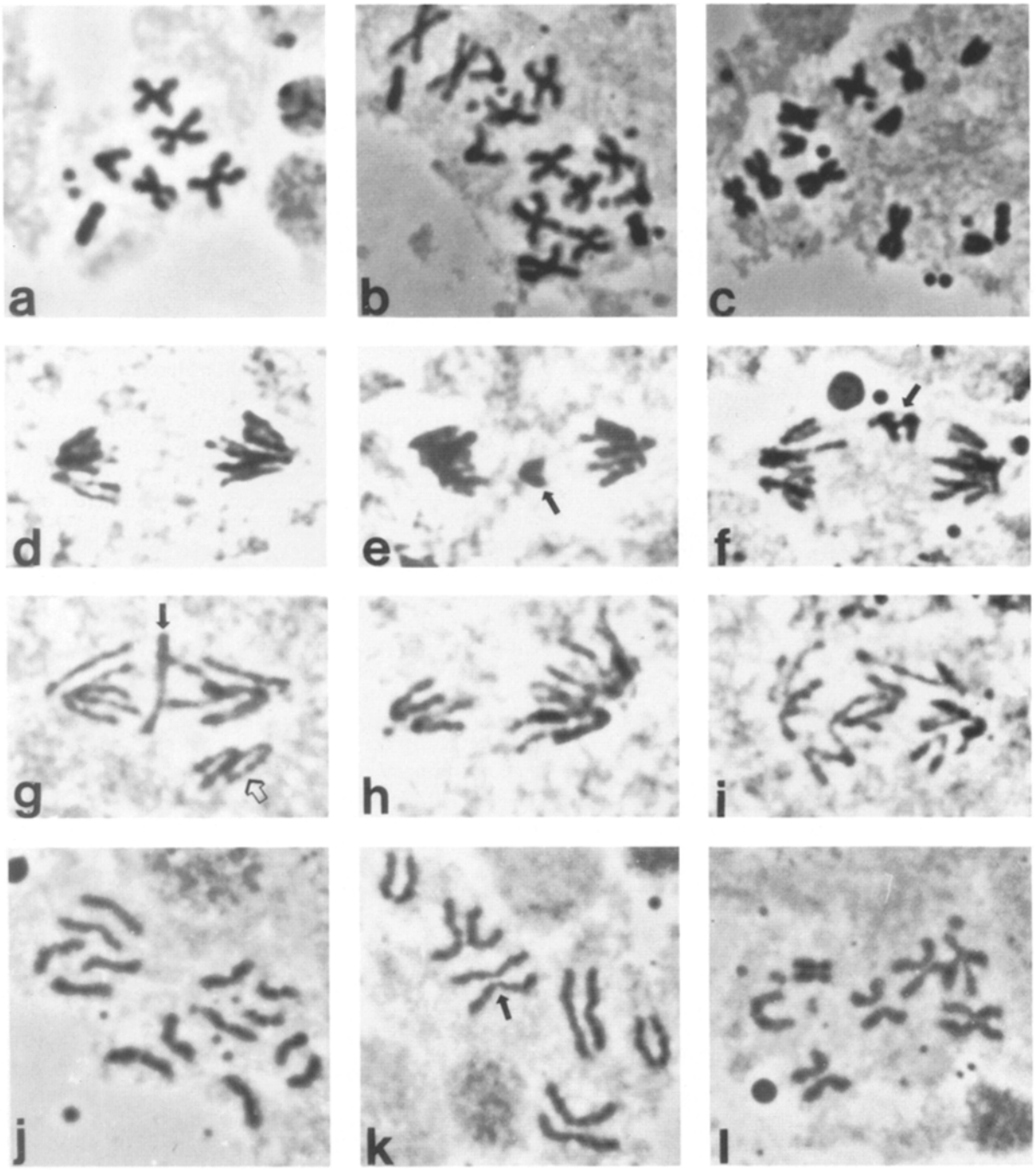

Figure 1. Cytological effects of *zw10* mutations in neuroblast cells. (*a–c*) Colchicine-treated metaphase figures. (*a*) Oregon R wild-type moles showing two pairs of metacentric autosomes, a telocentric X chromosome, a linear, heterochromatic Y chromosome (4A, XY), and two dot-like fourth chromosomes not scored in subsequent figures. (*b*) Adjacent aneuploid $zw10^{SI}$/Y cells (4A, XXY and 6A, XY). (*c*) 7A, 4XY $zw10^{i20}$/Y cell. (*d–i*) Anaphase figures from cells not treated with colchicine. (*d*) Oregon R wild type. (*e–f*) ($zw10^{i20}$/Y) Arrows denote lagging chromatid(s). (*g*) ($zw10^{S2M}$/Y) The open arrow shows a lagging sister chromatid pair; the black arrow indicates a chromatid apparently not subjected to poleward forces. (*h*) ($zw10^{SI}$/Y) Unequal anaphase. (*i*) ($zw10^{i20}$/Y) Disorganized anaphase. (*j–l*) Colchicine-treated metaphase figures showing precocious sister chromatid separation in $zw10^{i20}$/Y (*j* and *l*) and $zw10^{SI}$/Y (*k*) neuroblasts. In some cases, the apposition between sister chromatids, particularly at centromeric regions, remains close (*l*; arrow in *k*).

levels of aneuploidy observed in *zw10* mutant brain cells. They reported that in many colchicine-induced metaphase figures in mutant ganglia, sister chromatids appeared to be physically unconnected with each other. These investigators proposed that prematurely separated chromatids could establish connections at random to microtubules (MTs) emanating from the two spindle poles, and would thus segregate randomly at anaphase.

We have verified the occurrence of this form of precocious sister chromatid separation (PSCS). In the presence of col-

Table I. Aneuploidy in l(1)zw10 Mutant Brains

Genotype	Number of brains	Number of figures	4AXY	5AXY	4AXXY	4AXYY	6AXY	5AXXY	5AXYY	7AXY	Other	Percent aneuploid
$zw10^{65i20}/Y$	6	240	95	41	12	10	13	6	5	3	55	60.4
$zw10^{S2M}/Y$	7	232	104	36	18	11	8	4	3	2	46	55.1
$zw10^{S1}/Y$	6	323	147	53	24	19	9	5	6	1	59	54.5
X/Y (Oregon R)	10	1000	989	4	1	2	1	0	0	0	3	1.1

Neural ganglia from males hemizygous for the indicated *zw10* alleles or from wild-type Oregon-R males were dissected, incubated with colchicine, treated with hypotonic solution, fixed, stained, and squashed as described in Materials and Methods. *Number of brains* and *Number of figures* refer respectively to the total number of brains and the total number of colchicine-induced metaphase figures examined. The number of figures with particular karyotypes are listed. Because of difficulties in recognition of the small fourth chromosome, only the large second and third autosomes (A), which cannot be distinguished from each other, and the X and Y chromosomes were scored. Thus, the normal diploid male karyotype would be 4AXY. Similar results were obtained by Smith et al. (1985) for brains from individuals hemizygous for other *l(1)zw10* alleles.

chicine, 30–40% of *zw10* mutant nuclei display one or more chromatid pairs with PSCS (Table II). Sister chromatids are often adjacent to each other, yet appear unattached at their centromeres (Fig. 1, *j*, *k*, and *l*). Control ganglia from *C(1)DX, y f/Y* siblings of hemizygous mutants show PSCS at a frequency of <2%. Particular care was taken to ensure similar treatment of mutant and control brains. Both types of ganglia were dissected at the same time from animals grown in the same bottle; the brains were mixed and exposed to colchicine in the same vessel. Mutant and control brains were squashed together on the same slide; control ganglia can be recognized by the characteristic morphology of the attached X chromosome (see Materials and Methods). The absence of sister chromatid separation in wild-type, colchicine-treated *Drosophila* neuroblasts has also recently been noted by González et al. (1991).

Although the PSCS phenomenon is a characteristic of *zw10* mutants, the hypothesis of Smith et al. (1985) in its simplest form (see above) is unlikely to explain elevated levels of aneuploidy. First, *zw10* ganglia cells which have been subjected to neither colchicine nor hypotonic treatments do not show PSCS. Sister chromatids in these neuroblasts remain closely apposed to each other (data not shown); however, it is not clear whether or not the connection at the centromere is broken. A stronger argument is that random attachment of the chromatids to the spindle should not result in the lagging chromosomes or chromatids observed in anaphase figures (although figures with unequal numbers of chromosomes at the two poles would be apparent). We thus consider that PSCS is possibly an artefactual colchicine-dependent effect that may nonetheless reveal important differences between the centromeres of chromosomes in wild-type and mutant cells (see Discussion).

Other Mitotic Parameters. It is conceivable that the cytological effects of *zw10* mutations result from difficulties in progression through the cell cycle. For example, lagging chromatids appear at high frequencies after release of cells from a metaphase-arrested state (Hsu and Satya-Prakash, 1985). We have thus measured two parameters that provide some indication of the numbers of cells in various stages of mitosis. The mitotic index, an average of the number of cells undergoing mitosis per optic field, is similar in wild-type larval brains and in larval brains from a mutant that appears to represent the null state of the *zw10* locus (see below; Table II). In addition, the ratio between the number of cells in anaphase relative to the total number of mitotic figures is also not grossly affected by this mutation in *zw10* (Table II).

Tests for the Null Phenotype. To determine whether the phenotypes discussed above mirror the null state of the *zw10* gene, we have examined the cytological characteristics of

Table II. Mitotic Parameters of l(1)zw10 Mutant Brains

Genotype	Percent aberrant anaphases	PSCS	MI	Percent anaphase
$zw10^{65i20}/Y$	40.3 (149;9)	28.3 (956;6)	ND	ND
$zw10^{S2M}/Y$	38.6 (153;8)	40.4 (755;5)	ND	ND
$zw10^{S1}/Y$	47.4 (156;9)	30.0 (1136;7)	0.60	15.4 (2305;7)
C(1)DX,yf/Y	ND	1.1 (3000;15)	0.55	14.1 (2380;9)
X/Y (Oregon R)	3.2 (222;10)	1.8 (1000;5)	0.57	14.4 (3211;8)
$zw10^{S1}/Df(1)w^{rJ1}$	40.7 (22;2)	32.3 (295;2)	ND	ND

This table catalogs the results of three separate experiments. (*a*) The percentage of anaphases which appear abnormal is scored under *Percent aberrant anaphases*. This information was obtained from neural ganglia that were fixed and stained in the absence of colchicine or hypotonic treatments (see Materials and Methods). The first of the adjacent numbers, presented in smaller type and within parentheses, indicates the total number of anaphases scored; the second number refers to the number of brains examined. (*b*) *PSCS* shows the percentage of colchicine-induced, hypotonic-treated metaphase figures in which the centromeric connection between one or more pairs of sister chromatids appears to be severed. The larger of the adjacent numbers within parentheses indicates the total number of metaphase figures, the smaller, the total number of brains. (*c*) Brains fixed and stained without pretreatment (no colchicine or hypotonic incubations) were analyzed for mitotic index (*MI*) and percentage of total mitotic figures that are in anaphase (*Percent anaphase*). The mitotic index is expressed as the number of nuclei in division per optic field under standard conditions (see Gatti and Baker, 1989). As shown, hemizygosity for the $l(1)zw10^{S1}$ mutation has little effect on the mitotic index. For comparison, known mitotic mutants which result in few or no cells in division have mitotic indices two orders of magnitude lower than wild-type controls, while the mitotic index in brains of individuals carrying mutations causing metaphase arrest is 1.5–6 times higher than controls (Gatti and Baker, 1989). In the last column, both normal- and aberrant-appearing anaphases were combined. By visual inspection, ~40% of $l(1)zw10^{S1}/Y$ anaphases in this experiment were aberrant, in accord with the results from the independent experiment tabulated in the second column. For comparison, <0.6% of dividing cells are in anaphase in ganglia from known metaphase arrest mutants (Gatti and Baker, 1989). Adjacent numbers here refer to the total number of optic fields and the number of brains examined (see Materials and Methods).

larvae heterozygous for a deletion ($Df(1)w^{rJ1}$) that removes *zw10* and for a *zw10* mutant allele. Levels of hyperploidy (52.1% [74/142 nuclei] for $zw10^{65i20}/Df(1)w^{rJ1}$ and 49.6% [64/129] for $zw10^{S1}/Df(1)w^{rJ1}$) were similar to values observed in *zw10* hemizygous animals (compare with Table I). Both frequencies of aberrant anaphases and PSCS in $zw10^{65i20}/Df(1)w^{rJ1}$ mitotic figures were also close to values seen for the mutant alleles alone (Table II). If the *zw10* alleles examined were hypomorphic, it would be expected that deficiency/mutant heterozygotes would display a stronger phenotype than animals homozygous or hemizygous for the mutation alone. These classical genetic tests therefore suggest that the mutations we have analyzed, all of which have similar effects, characterize the null state of the *zw10* gene; this hypothesis is supported by analysis of the *zw10* protein in mutant animals, as reported below.

Molecular Mapping of the zw10 Locus

A portion of the *Drosophila* X chromosome including the *zw10* gene was cloned during the course of a chromosomal walk through the *zeste-white* interval (Goldberg et al., 1983; Gunaratne et al., 1986; our own unpublished data). Within this region, *zw10* must be located distal (relative to the centromere) of the deletion *Df(1)64j4*, and completely within the duplication $Dp(1;2)w^{+70h31}$ (Fig. 2). The locations of the breakpoints associated with these two rearrangements were ascertained by whole genomic Southern blots and by in situ hybridization to salivary gland polytene chromosomes from larvae of the appropriate genotype (Fig. 2; data not shown). These results delimit *zw10* to a region of 11 kb within the cloned X chromosome interval.

Two observations suggested that part of the *zw10* locus must lie near the $Dp(1;2)w^{+70h31}$ breakpoint at coordinate −0.3 on Fig. 2. First, the genetic map distance between *zw10* and the adjacent lethal complementation group *zw4* is very small (<0.026 map units, or <7.8 kb based on a conversion of 1 map units = 300 kb in this region of the X chromosome) (Kidd et al., 1983), yet $Dp(1;2)w^{+70h31}$ encompasses *zw10* but not *zw4*. Second, a spontaneous allele, $zw10^{S1}$ (Schalet, 1986), is associated with a 4.5-kb insertion of DNA at coordinate +1.7. This DNA insertion in $zw10^{S1}$ is most likely a *Doc* mobile element, based on the similarity of their restriction maps (Driver et al., 1989).

Northern blot analysis of adult poly(A)+ mRNA re-

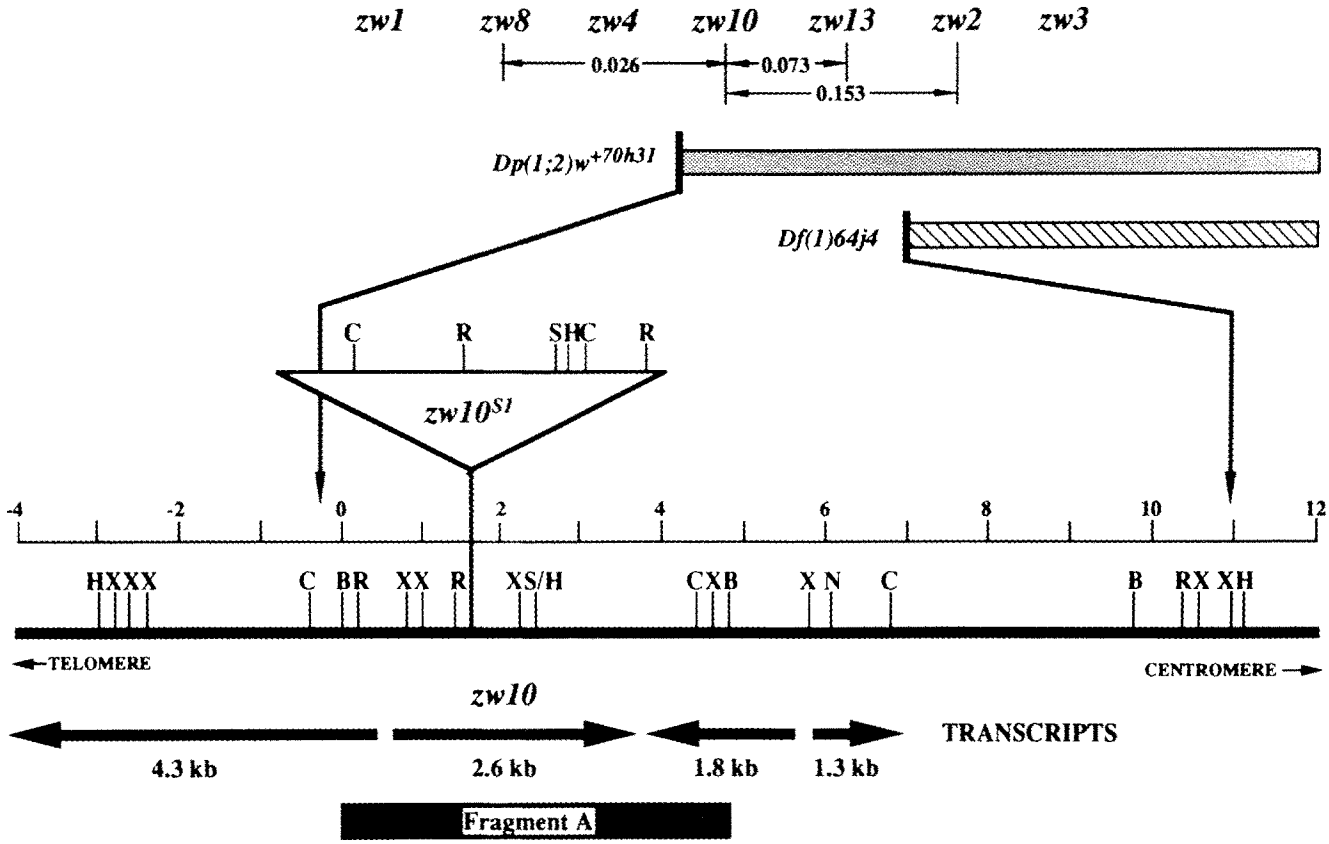

Figure 2. Genetic and molecular map of the *zw10* region. Lethal complementation groups in the vicinity of *l(1)zw10* are shown at the top of the figure, distances between genes are given in centimorgans (Judd et al., 1972). (▩) Loci contained within the duplication $Dp(1;2)w^{+70h31}$; genes deleted in *Df(1)64j4* are indicated by the hatched bar. The molecular map is shown only for a 16-kb region immediately adjacent to the *zw10* gene; coordinates are given in kb, with 0 defined as the *BamHI* site at the left end of Fragment A used to rescue *zw10* phenotypes (see text). The mobile element in $zw10^{S1}$ is diagrammed to the same scale as the remainder of the restriction map. The direction of transcription producing poly(A)+ RNAs from this region is shown by arrows; the sizes of mature transcripts are indicated below. *H*, *Hind*III; *X*, *Xho*I; *B*, *Bam*HI; *R*, *Eco*RI; *C*, *Sac*I; *N*, *Not*I; and *S*, *Sal*I.

vealed a 2.6-kb transcript located just proximal to the *Dp(1;2)w*$^{+70h31}$ breakpoint and that spanned the site of the *zw10*^{S1} insertion element (Fig. 2); this was therefore a likely candidate for the *zw10* mRNA. A 4.8-kb fragment of genomic DNA (Fragment A: coordinates 0–4.8 on Fig. 2), encoding the entire 2.6-kb transcript but containing no other complete transcriptional unit, was transformed into *Drosophila* by P element-mediated germline transformation. This fragment, as present in three independent autosomal transformant lines, is necessary and sufficient to rescue the lethal phenotype of several *zw10* alleles (Materials and Methods). Fragment A also repairs the *zw10* mitotic phenotype. For example, in rescued *zw10*^{S2M}*/Y; P[Fragment A]/+* larval ganglia, the frequency of aneuploidy (1.2%) and PSCS (4.3%) were at wild type levels (compare with Table II), while anaphases were normal (not shown). Thus, the entire *zw10* locus must reside within the 4.8-kb Fragment A depicted in Fig. 2, and appears to be transcribed into a poly(A)+ RNA 2.6 kb in length.

Molecular Analysis of the zw10 Locus

The *zw10* transcript is developmentally regulated. The highest levels of this RNA are found in embryos and in adult females (Fig. 3), consistent with the idea that maternally supplied *zw10* supports the rapid syncytial divisions of early embryogenesis. Levels of *zw10* RNA are substantially decreased during the first and second larval instar, but then increase in third instar larvae and in early pupae. Presumably, this reflects the increased number of proliferating cells in late larval/early pupal imaginal discs. Only a single 2.6-kb RNA band is seen at any stage of development on Northern blots; it nonetheless remains possible that alternatively processed species of similar length, or rare RNAs of different sizes, may be produced from the same transcriptional unit.

Three cDNA clones homologous to the 2.6-kb *zw10* mRNA were isolated from an imaginal disc cDNA library (Brown and Kafatos, 1988). Substantial overlap in the restriction maps of these cDNAs suggests that they all represent the same species (data not shown). The sequence of the longest of these cDNAs (2,576 bp) contains an open reading frame beginning at nucleotide 103 that encodes a protein of 721 amino acids (Fig. 4). However, it should be cautioned that the nucleotides in the vicinity of this putative initiation codon show only partial agreement with the *Drosophila* translation start consensus (C A C/A C/A AUG; Cavener and Ray, 1991). Better matches are seen in the vicinity of the downstream methionine codons at nucleotide positions 232–235, 343–345, and 400–402. Although it is thus possible that translation of the corresponding mRNA may initiate at any of these positions, the size of the *zw10* protein (see below) is most consistent with use of the codon indicated in Fig. 4.

A computerized search has failed to reveal significant homologies to any protein within the Genbank, EMBL, PIR, and Swiss-Prot databases. Given the cell cycle-dependent changes in the intracellular location of *zw10* protein that will be described below, it is of interest that the *zw10* sequence contains motifs that may be subject to phosphorylation. A potential tyrosine kinase phosphorylation site (consensus sequence R/K [2,3] D/E [2,3] Y) is found beginning at amino acid 48, while sites possibly available for phosphorylation by the *cdc2* kinase (TP and SP) start at amino acids 63 and 167 (Shalloway and Shenoy, 1991).

Antibodies Against the zw10 Protein

Polyclonal rabbit antibodies were generated against gel-purified β-galactosidase–*zw10* fusion protein (β-gal–*zw10*) that had been produced in *E. coli* cells. Crude antisera were purified by immunoaffinity chromatography against *trpE–zw10* protein fusions (see Materials and Methods for further information concerning the preparation and characterization of these reagents). The purified antibodies recognize a single band of 85 kD, consistent with the size of the predicted *zw10* protein, in Western blots of 0–16-h old embryos, of third instar larvae, and of *Drosophila* Schneider Line 2 tissue culture cells (Fig. 5, *A* and *B*). When the same Schneider cell line is transfected with a construct containing the complete *zw10* open reading frame under the control of the strong

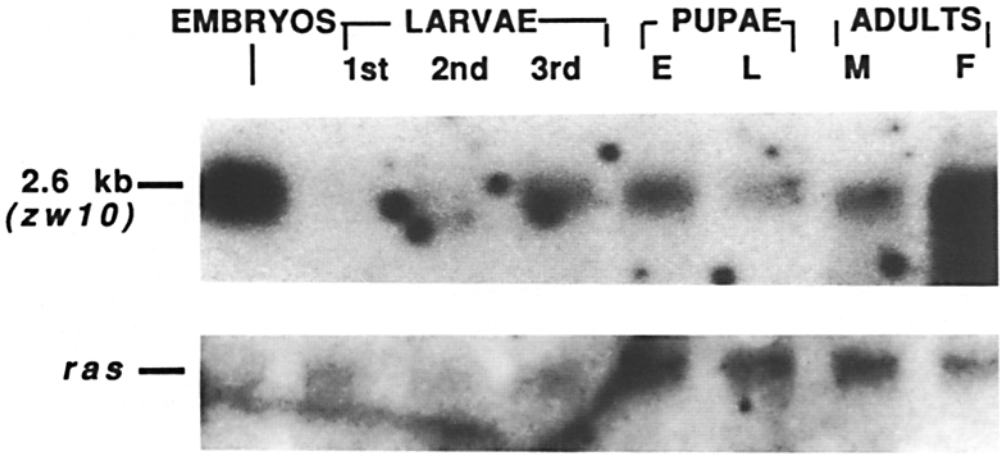

Figure 3. Developmental regulation of the *zw10* transcript. The poly(A)+RNA fractions from various stages (0–24-h embryos, first, second, and third larval instars, light early pupae [*E*] and dark late pupae [*L*], adult males [*M*] and adult females [*F*] were isolated (see Materials and Methods). In the blot shown, 10 μg of poly(A)+RNA was loaded in each lane. The *zw10* probe used was a fragment containing the full-length *zw10* cDNA, and hybridizes to a single 2.6-kb transcript. Hybridization of the same Northern blot with a probe prepared from *Dmras-64BA* (*ras*) (Mozer et al., 1985) to control for loading is shown below.

```
   1  GGCTTTTTTGAACAATCGTTGGTAGCAACAGGGAATTGCAGAAACCAGTTGTCTTGGGTTTCGCAAGAATTGGAAAAGGAGGATCTGGTCAAAGAGCAGGAC   102

 103  ATGGAGGAAGAGGCGCCGCGGTTCAATGTGCTGGAGGAGGCGTTCAACGGCAATGGGAACGGGTGCGCCAACGTGGAGGCCACCCAATCGGCCATATTAAAA   204
   1  M  E  E  E  A  P  R  F  N  V  L  E  E  A  F  N  G  N  G  N  G  C  A  N  V  E  A  T  Q  S  A  I  L  K    34

 205  GTGCTGACGCGCGTTAATCGCTTCCAGATGCGCGTCCGCAAGCACATCGAAGACAACTACACGGAGTTTATGCCCAACAACACGTCGCCGGACATATTTCTG   306
  35  V  L  T  R  V  N  R  F  Q  M  R  V  R  K  H  I  E  D  N  Y  T  E  F  M  P  N  N  T  S  P  D  I  F  L    68

 307  GAGGAGTCGGGGTCCTTGAATCGCGAGATTCACGACATGCTCGAGAACTTGGGCTCCGAGGGACTGGACGCCTTGGACGAGGCGAATGTCAAGATGGCGGGT   408
  69  E  E  S  G  S  L  N  R  E  I  H  D  M  L  E  N  L  G  S  E  G  L  D  A  L  D  E  A  N  V  K  M  A  G    102

 409  AACGGCAGGCAGCTGCGAGAGATCCTTTTGGGTCTGGGTGTCAGCGAGCATGTGCTAAGGATCGACGAGCTGTTCCAGTGCGTGGAGGAGGCCAAGGCCACC   510
 103  N  G  R  Q  L  R  E  I  L  L  G  L  G  V  S  E  H  V  L  R  I  D  E  L  F  Q  C  V  E  E  A  K  A  T    136

 511  AAGGATTACTTGGTGTTACTGGACCTTGTCGGTCGTTTGAGGGCTTTCATCTATGGCGATGATTCCGTTGACGGGGACGCGCAGGTGGCCACGCCAGAGGTT   612
 137  K  D  Y  L  V  L  L  D  L  V  G  R  L  R  A  F  I  Y  G  D  D  S  V  D  G  D  A  Q  V  A  T  P  E  V    170

 613  CGACGCATCTTTAAGGCTCTCGAGTGCTACGAGACCATCAAGGTGAAATACCATGTACAGGCATATATGCTGCAGCAGAGCCTCCAGGAGCGCTTCGCTCGC   714
 171  R  R  I  F  K  A  L  E  C  Y  E  T  I  K  V  K  Y  H  V  Q  A  Y  M  L  Q  Q  S  L  Q  E  R  F  A  R    204

 715  CTGGTGCAGCTGCAGTGTAAATCCTTTCCCACATCGCGTTGCGTCACCTTGCAGGTGAGCCGGGATCAAACGCAGCTGCAGGATATTGTGCAGGCTCTCTTC   816
 205  L  V  Q  L  Q  C  K  S  F  P  T  S  R  C  V  T  L  Q  V  S  R  D  Q  T  Q  L  Q  D  I  V  Q  A  L  F    238

 817  CAGGAGCCCTACAATCCGGCGCGCCTCTGCGAATTCCTGCTGGACAATTGCATAGAACCGGTGATCATGCGCCCAGTGATGGCCGATTACAGCGAAGAAGCC   918
 239  Q  E  P  Y  N  P  A  R  L  C  E  F  L  L  D  N  C  I  E  P  V  I  M  R  P  V  M  A  D  Y  S  E  E  A    272

 919  GATGGTGGCACCTACGTTCGATTGTCGCTTTCCTACGCCACCAAGGAGCCCAGCTCAGCGCACGTTCGCCCGAACTACAAGCAGGTCTTGGAGAACCTCAGG  1020
 273  D  G  G  T  Y  V  R  L  S  L  S  Y  A  T  K  E  P  S  S  A  H  V  R  P  N  Y  K  Q  V  L  E  N  L  R    306

1021  CTGCTGCTGCACACGCTGGCCGGGATCAACTGCAGTGTGTCCAGGGACCAACATGTTTTTGGCATTATTGGCGATCATGTGAAGGATAAAATGCTGAAATTA  1122
 307  L  L  L  H  T  L  A  G  I  N  C  S  V  S  R  D  Q  H  V  F  G  I  I  G  D  H  V  K  D  K  M  L  K  L    340

1123  CTGGTGGACGAGTGCCTGATACCAGCTGTGCCCGAAAGCACGGAGGAGTATCAGACATCCACGCTGTGTGAGGATGCCGCCCAGCTGGAGCAGCTGCTTGTA  1224
 341  L  V  D  E  C  L  I  P  A  V  P  E  S  T  E  E  Y  Q  T  S  T  L  C  E  D  A  A  Q  L  E  Q  L  L  V    374

1225  GACTCATTCATCATCAATCCCGAGCAAGATCGAGCCCTAGGGCAGTTTGTAGAGAAGTACGAGACCTACTACCGCAATCGGATGTATCGTCGAGTTCTGGAA  1326
 375  D  S  F  I  I  N  P  E  Q  D  R  A  L  G  Q  F  V  E  K  Y  E  T  Y  Y  R  N  R  M  Y  R  R  V  L  E    408

1327  ACGGCGCGGGAGATCATCCAGCGCGATCTGCAGGACATGGTGCTGGTGGCGCCCAACAACCACTCAGCCGAAGTGGCAAACGATCCCTTCCTCTTCCCACGC  1428
 409  T  A  R  E  I  I  Q  R  D  L  Q  D  M  V  L  V  A  P  N  N  H  S  A  E  V  A  N  D  P  F  L  F  P  R    442

1429  TGCATGATCTCGAAAAGTGCTCAGGACTTTGTCAAACTAATGGACCGCATTCTTCGCCAGCCCACGGATAAACTGGGCGACCAAGAGGCCGATCCCATAGCC  1530
 443  C  M  I  S  K  S  A  Q  D  F  V  K  L  M  D  R  I  L  R  Q  P  T  D  K  L  G  D  Q  E  A  D  P  I  A    476

1531  GGCGTCATTTCCATCATGCTGCACACCTACATCAATGAGGTGCCCAAGGTGCACCGCAAGCTGCTCGAGAGCATTCCACAGCAGGCCGTCCTGTTCCACAAC  1632
 477  G  V  I  S  I  M  L  H  T  Y  I  N  E  V  P  K  V  H  R  K  L  L  E  S  I  P  Q  Q  A  V  L  F  H  N    510

1633  AATTGTATGTTCTTCACACACTGGGTAGCGCAGCATGCGAACAAGGGCATCGAAAGCTTGGCGGCGCTGGCCAAGACACTGCAGGCCACCGGTCAGCAGCAT  1734
 511  N  C  M  F  F  T  H  W  V  A  Q  H  A  N  K  G  I  E  S  L  A  A  L  A  K  T  L  Q  A  T  G  Q  Q  H    544

1735  TTCCGCGTGCAGGTCGACTACCAATCCTCCATCCTGATGGGCATCATGCAGGAGTTCGAGTTCGAGAGCACGCACACGCTGGGCTCTGGTCCACTGAAGCTG  1836
 545  F  R  V  Q  V  D  Y  Q  S  S  I  L  M  G  I  M  Q  E  F  E  F  E  S  T  H  T  L  G  S  G  P  L  K  L    578

1837  GTGCGTCAGTGCCTTCGCCAGCTGGAGCTGCTGAAGAACGTGTGGGCCAATGTGCTCCCGGAGACCGTGTACAATGCAACCTTCTGCGAGCTAATCAACACA  1938
 579  V  R  Q  C  L  R  Q  L  E  L  L  K  N  V  W  A  N  V  L  P  E  T  V  Y  N  A  T  F  C  E  L  I  N  T    612

1939  TTTGTCGCCGAGCTAATCCGTCGAGTGTTCACGCTGCGCGACATTTCCGCACAGATGGCCTGTGAGCTGAGCGATCTCATTGACGTGGTGCTCCAGCGGGCG  2040
 613  F  V  A  E  L  I  R  R  V  F  T  L  R  D  I  S  A  Q  M  A  C  E  L  S  D  L  I  D  V  V  L  Q  R  A    646

2041  CCCACGCTTTTCCGCGAACCAAACGAGGTGGTCCAGGTGCTCTCTTGGCTTAAGCTGCAGCAACTGAAGGCCATGCTGAACGCGTCGCTCATGGAGATCACA  2142
 647  P  T  L  F  R  E  P  N  E  V  V  Q  V  L  S  W  L  K  L  Q  Q  L  K  A  M  L  N  A  S  L  M  E  I  T    680

2143  GAGCTGTGGGGCGACGGCGTCGGCCCGCTGACCGCCAGCTACAAGTCGGATGAGATAAAGCACCTAATCAGGGCGTTGTTCCAGGATACGGATTGGCGGGCC  2244
 681  E  L  W  G  D  G  V  G  P  L  T  A  S  Y  K  S  D  E  I  K  H  L  I  R  A  L  F  Q  D  T  D  W  R  A    714

2245  AAGGCCATTACGCAGATTGTATAGGGCGCGTGCGTTTTTTGCGAGCGAGGAATGTTGAACAGCGGATAGACATCACATTTGAGGTGGTAAACGGAGTCTAAA  2346
 715  K  A  I  T  Q  I  V  *  721

2347  TTTGATGATCACCATCAATGTGTTCTACTTAATTCCTTGAATGTTTACCACAATGGGAAAAGTAATAGAATTTGATAATCTTTAATTCTCCGAATGGTTTCT  2448

2449  TGTTGTACATAGAAAAGTAATTATCCACAAAAACCATTCCATTCTTCCCGCAACGCAACACAATATTTACTTAAGACTTATTTAAATGAATAAAAACAACTA  2550

2551  AATCCCATTAAAAAAAAAAAAAAAAA  2576
```

Figure 4. Sequence of the *zw10* cDNA. The nucleotide sequence of the coding strand of the longest *zw10* cDNA clone, with position 1 assigned to the 5′-most base. The ATG at 103 is the most likely site of initiation, but other ATGs (at 232, 343, and 400) are also possible choices (see text). A stop codon (*TAG*) at position 2,268 has been signified by an *asterisk*. The sequence is thus postulated to contain a 5′-untranslated region from nucleotides 1–102, and a 3′-untranslated region from nucleotides 2,269–2,576. A single long open reading frame encodes a predicted protein sequence, here represented by the single-letter code, of 721 amino acids in length, having a molecular weight of 82,115. These sequence data are available from EMBL/GenBank/DDBJ under accession number X64390.

actin5C promoter (Bond and Davidson, 1986), this same band is clearly overproduced (Fig. 5 *A*).

Evidence that the antibody reacts specifically with the *zw10* gene product is provided by the analysis of extracts from larvae hemizygous for mutant *zw10* alleles. The $zw10^{S1}$ and $zw10^{65.20}$ mutants have no detectable 85-kd *zw10* protein (Fig. 5 *B*). The $zw10^{S1}$ allele does not appear to encode stable *zw10* cross-reactive polypeptides, and is thus likely to represent the null state of the locus. This result is expected, because the $zw10^{S1}$ gene is interrupted by a DNA insertion (Fig. 2). These exogenous sequences are located within an exon near the middle of the coding sequence (see Materials and Methods), between nucleotides 1,220 and 1,375 (Fig. 4). Males of genotype $zw10^{65.20}$/Y display a band of ~75 kD that we presume to be a truncated product caused by a nonsense or frameshift mutation; the amount of this 75-kD protein is reduced relative to the amount of 85-kD *zw10* protein in wild type (Fig. 5 *B*).

Immunolocalization of the zw10 Antigen

To determine the location of *zw10* protein at different stages of the cell cycle, we chose to examine mitosis in syncytial blastoderm embryos by indirect immunofluorescence using

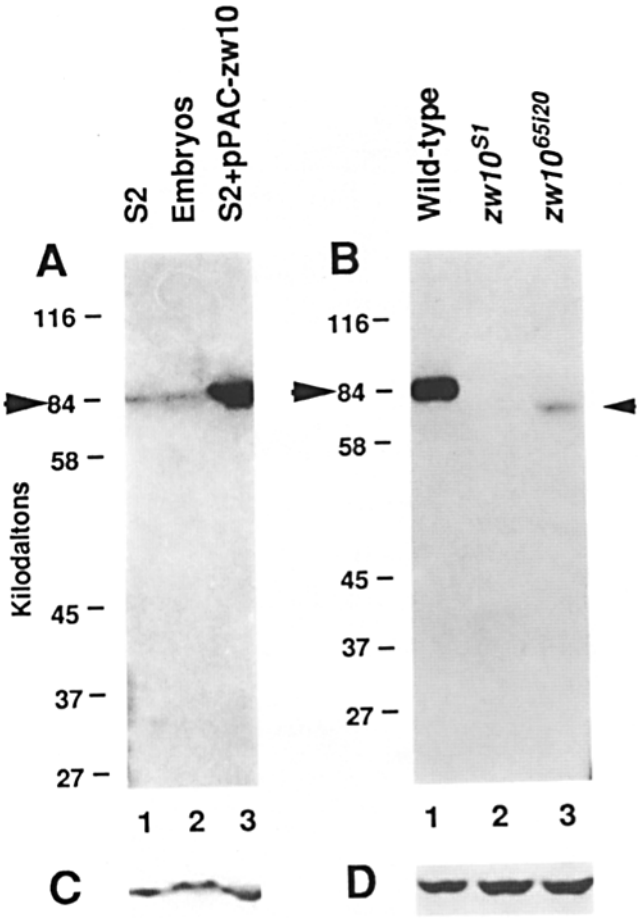

Figure 5. Detection of the *zwl0* protein on Western Blots. (*A*) The *zwl0* protein is recognized by purified antibodies. Protein extracts from *Drosophila* Schneider Line 2 tissue culture cells (*S2*), 0–16-h-old embryos, and Schneider cells transfected with a construct placing the *zwl0* cDNA under the control of the high-level *actin5C* promoter (*S2+pPAC-zwl0*) were subjected to SDS-PAGE and blotted, followed by detection with an affinity-purified polyclonal antibody to *zwl0* epitopes (see Materials and Methods). The 84-kd *zwl0* protein (*arrowhead, left*) is overexpressed when pPAC-*zwl0* is transfected into S2 cells. (*B*) The *zwl0* protein is altered in *zwl0* mutants. In wild-type larvae (lane *1*) the *zwl0* protein appears as a single band of 85 kd (*arrowhead, left*). In $zwl0^{S1}$ larvae, there is no detectable protein of this size present (lane *2*). In $zwl0^{65i20}$ larvae (lane *3*), protein of the wild type size is also not observed, and is replaced by a cross-reacting protein of ~75 kD present in lower abundance (*smaller arrowhead, right*). Total protein from two third-instar male larvae of the appropriate genotype was loaded in each lane. Anti-*zwl0* crude serum was diluted 1/700. (*C* and *D*) Reaction of the filters depicted in *A* and *B*, respectively, with antibody to a 54-kD *Drosophila* protein (R. Gandhi and M. L. Goldberg, manuscript in preparation) as a loading control.

the purified antibodies described above. Distinctive patterns are observed at different stages of mitosis. The progression of these *zwl0* staining patterns through the cell cycle is also identical in the mitotic domains of cellularized embryos (Foe, 1989) and in larval neuroblast cells, so the observed distribution of *zwl0* protein is not specific to syncytial blastoderm stages 9–13 (data not shown).

Prometaphase to Metaphase. During interphase and most of prophase, the *zwl0* protein appears to be excluded from the nucleus (see below). At a time we assume corresponds to the partial breakdown of the nuclear envelope at the beginning of prometaphase (Stafstrom and Staehelin, 1984; Hiraoka et al., 1990), *zwl0* antigen starts to coalesce in the nuclear domain (Fig. 6, *a* and *d*). The staining is mostly amorphous and surrounds the condensing chromosomes, but a few discrete spots appear to be recognized by the antibody.

By metaphase, *zwl0* protein becomes localized to discrete, filamentous structures residing in the central, longitudinal portion of the spindle (Fig. 6, *b* and *e*; Fig. 7, *A–C*). The strands originate near the centrosomes at opposite poles of the spindle apparatus, but *zwl0* staining of the centrosomes per se is not observed (Fig. 7 *B*). Remarkably, and in contrast with the total tubulin pattern, *zwl0* antigen appears to pass directly through the chromosomal mass at the metaphase plate (Fig. 7, *A* and *C*).

Anaphase. At the beginning of anaphase, *zwl0* antigen becomes excluded from the region of the metaphase plate, and the filaments shorten from their ends nearest the centrosomes. As a result, *zwl0* protein becomes concentrated into punctate structures at the leading edges of the separated chromatids (Fig. 6, *c* and *f*; Fig. 7, *D–F*). At this level of resolution, the number and position of these structures is consistent with localization at the centromere/kinetochore region of individual chromatids. The *zwl0* protein appears to remain at or near the kinetochores through the remainder of anaphase, although the shortening of kinetochore microtubules (KMTs) at these later stages of anaphase renders resolution in the kinetochore–centrosome interval difficult (Fig. 6, *g* and *j*).

The transition between the metaphase and early anaphase states of *zwl0* is very rapid. Mitosis in syncytial *Drosophila* embryos is metasynchronous: division starts at successively later times in nuclei increasingly closer to the embryonic equator, forming a mitotic wave (Foe and Alberts, 1983). As seen in Fig 8, adjacent nuclei can display the mature metaphase and anaphase *zwl0* patterns, but intermediate structures are sometimes observed. Although the rate of mitotic wave propagation is quite variable, at an average value of 100 μm/min (Foe and Alberts, 1983), and given the approximate distance between adjacent nuclei (~20 μm at blastoderm stages 11–12), we estimate that the transition between the metaphase and anaphase states of *zwl0* may be accomplished in periods as short as 10–12 s.

Telophase, Interphase, and Prophase. At the beginning of telophase, the *zwl0* antigen becomes excluded from the domain of the reforming nucleus (Fig. 6, *h* and *k*). Staining is also restricted to the extranuclear cytoplasm during interphase (Fig. 6, *i* and *l*) and prophase (not shown).

Discussion

zwl0 Mutations Affect Chromosome Segregation

Several observations indicate that $zwl0^{+}$ function is necessary to ensure accurate chromosome segregation during cell division in most, if not all, *Drosophila* tissues. (*a*) A temperature-sensitive mutation of *zwl0* ($zwl0^{ts}$) caused a 120-fold increase in the incidence of clones of homozygous *multiple wing hair (mwh)* cells in the wings of $zwl0^{ts}/Y$; *mwh*/+ males raised at semi-restrictive temperature. Additional tests implicated an elevated frequency of mitotic non-

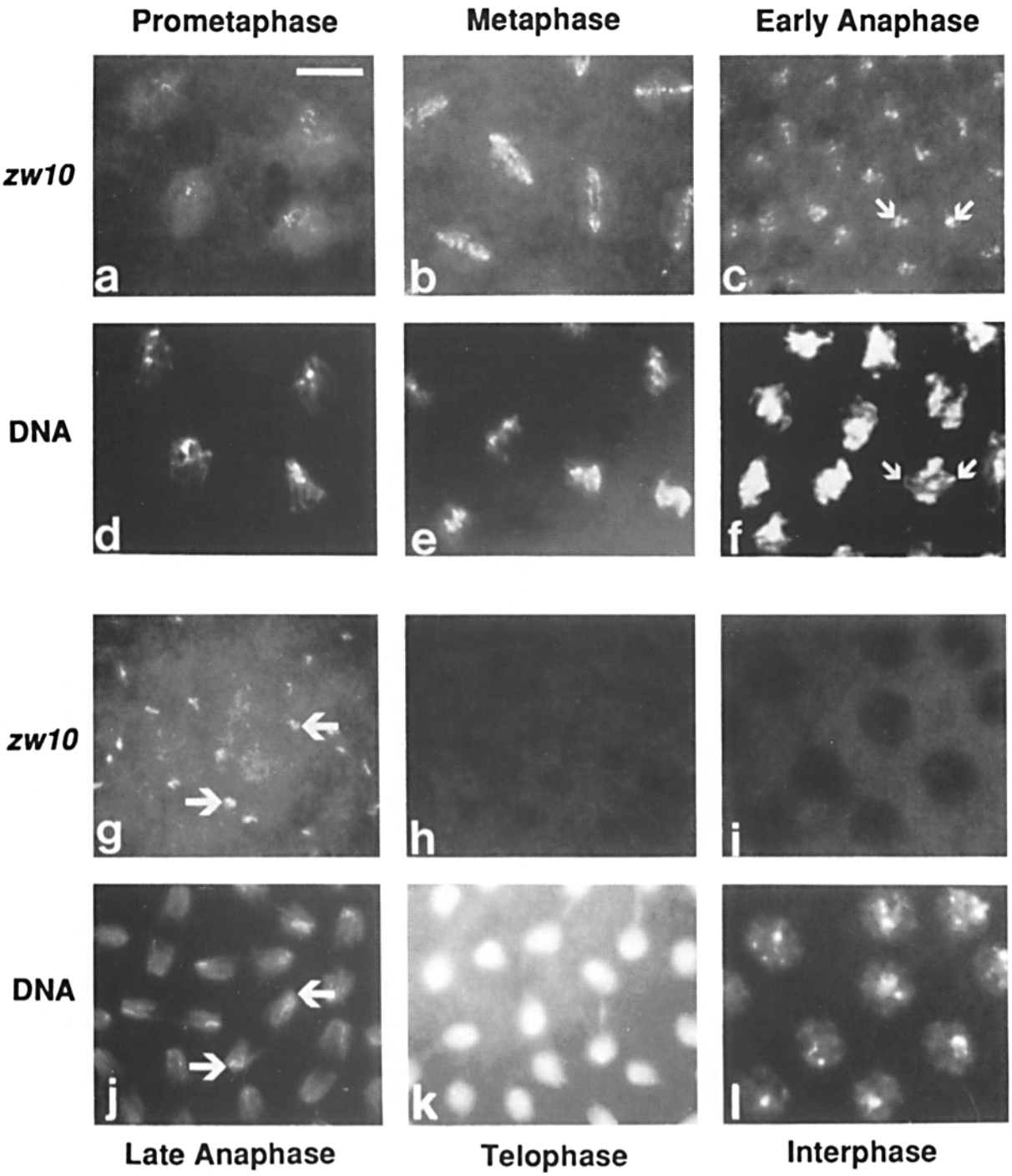

Figure 6. Immunolocalization of the *zwl0* protein during the cell cycle in wild-type syncytial blastoderm embryos. Embryos were fixed, stained, and processed for indirect immunofluorescence as described (see Materials and Methods). (*a–c* and *g–i*) *zwl0* protein localization is shown; below each of these is shown the corresponding DNA staining (*d–f* and *j–l*). (*a* and *c*) Prometaphase; *zwl0* protein moves into the nuclear domain; punctate staining is visible. (*b* and *e*) Metaphase; *zwl0* filamentous strands are completely formed; considerable substructure is apparent. (*c* and *f*) Anaphase; *zwl0* protein is rapidly relocalized to the kinetochore regions of separating sister chromatids (*arrows*). (*g* and *j*) Late anaphase; *zwl0* protein remains on kinetochores (*arrows*). (*h* and *k*) Telophase; *zwl0* antigen disappears from kinetochores. Faint cytoplasmic staining is apparent. (*i* and *l*) Interphase; no nuclear localization is visible. Bar, 10 μm.

disjunction in the formation of these somatic clones (Smith et al., 1985). (*b*) As discussed above, a high proportion of *zwl0* mutant larval brain neuroblast cells are aneuploid. Many anaphase figures in these cells are obviously aberrant. (*c*) Upon completion of the second meiotic division in escaper males, spermatid nuclei containing different numbers of chromosomes are produced (our own unpublished observations). It is not presently clear whether missegregation occurs during the first or second meiotic divisions, or during earlier mitoses in the male germline. (*d*) Maternally supplied *zwl0* gene product is necessary for embryogenesis, as shown by germline clonal analysis (Perrimon et al.,

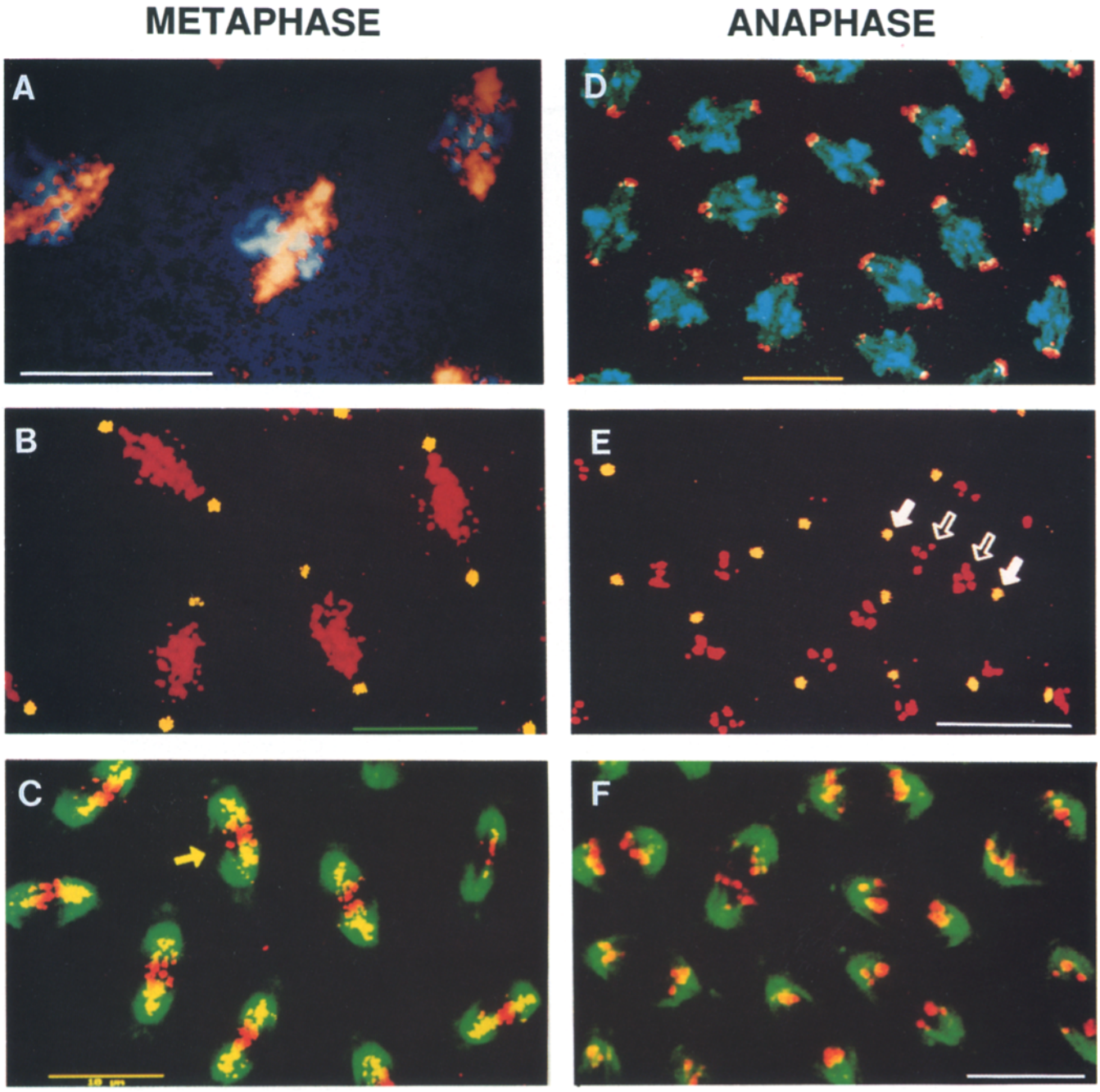

Figure 7. Localization of *zw10* protein in comparison with chromosomes, centrosomes, and tubulin. The embryos were processed for indirect immunofluorescence and confocal microscopy as outlined in the Materials and Methods. Superimposed images were obtained from the same focal plane. (*A*) At metaphase, *zw10* protein (*orange*) filaments extend through the chromosomal mass (*blue*) and have considerable substructure (particularly apparent in the nucleus at far left). (*B*) Centrosomes (*yellow*) and the *zw10* protein (*red*) at metaphase. *zw10* protein filaments extend to, but do not overlap with, centrosomes. (*C*) Tubulin staining (*green*) and *zw10* protein (*red*) at metaphase. The *zw10* protein is localized to only a subsection of the mitotic spindle (*arrow*; regions of overlap between *zw10* and tubulin are *yellow*.) (*D*) Regions in or near kinetochores of chromosomes (*blue*) are the sites of *zw10* protein localization (*red*) during early–mid anaphase. (*E*) At early anaphase, centrosomes (*yellow*; *solid arrows*) are well resolved from *zw10* (*red*; *outline arrow*). (*F*) *zw10* (*red*) is restricted to discrete spots at the centrosome-distal portion of each hemispindle at anaphase onset (tubulin staining is *green* while overlap is *yellow*). Thus, *zw10* is not found along the length of the KMTs at this stage of the cell cycle. Bars, 10 μm.

1989). In addition, syncytial blastoderm embryos derived from *zw10* escaper females (see below) have abnormally spaced nuclei of aberrant morphology (our own unpublished results).

These findings may be understood in terms of the varying requirements for cell division at different stages in *Drosophila* development. Maternally derived gene products within the egg must be used to construct the molecular machinery required for the rapid embryonic mitoses after fertilization, because little transcriptional activity occurs during this period. For many proteins involved in mitosis, the maternal contribution is sufficient to allow development into larval

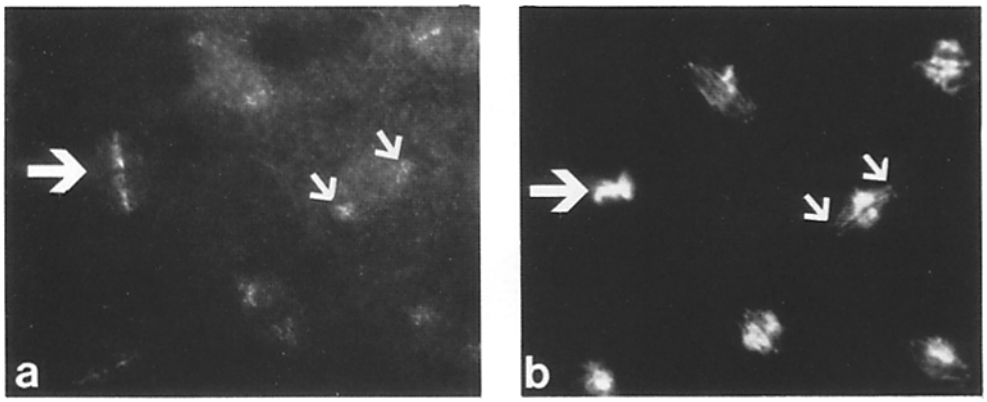

Figure 8. Rapid relocalization of the *zw10* protein. (*a*) *zw10* antigen staining; the corresponding DNA staining is presented in *b*. Metaphase *zw10* protein strands (*large arrow* at left) are replaced in an adjacent nucleus by kinetochore region staining (*smaller arrows* to the right) at anaphase.

stages (Gatti and Baker, 1989). Larval growth per se is accomplished through an increase in cell size, accompanied in some tissues by polytenization. Cell division within the larva is in general restricted to tissues that will play a role in subsequent adult morphogenesis: the nervous system, imaginal discs, and abdominal histoblasts.

The phenotype of *zw10* mutants is consistent with this picture. Because sufficient *zw10* product is supplied by *zw10*/+ heterozygous mothers, *zw10* embryos can survive as larvae. However, zygotic expression of *zw10* in the larval tissues enumerated above would be necessary for further development. Mitosis in larval brain neuroblasts and the imaginal disks giving rise to the adult cuticle would therefore be abnormal, resulting in substantial late larval/pupal lethality (Gatti and Baker, 1989). On the other hand, effects of *zw10* mutations on embryogenesis would only be observed when *zw10* protein within the egg is depleted, as in eggs produced by homozygous escaper females.

Cytological Effects of zw10 Mutations

The evidence presented above clearly shows that mutations in the *zw10* gene cause aberrant anaphases within larval neuroblasts, in turn generating a high proportion of aneuploid brain cells. We have also verified that the phenomenon of PSCS is an additional consequence of *zw10* lesions in colchicine-treated neural ganglia. However, the proposition that the anaphase defects observed are due to PSCS before anaphase onset remains questionable, because of uncertainties about the state of cells exposed to colchicine and because of our lack of knowledge concerning the forces that determine sister chromatid interactions.

The consideration of published precedents for the cytological phenotypes discussed above may be instructive in speculations concerning potential functions of the *zw10*$^{+}$ protein. Lagging sister chromatids have been postulated to result from damage to the centromere/kinetochore produced by drugs (Brinkley et al., 1985; Hsu and Satya-Prakash, 1985), by injection with anticentromere antibodies (Bernat et al., 1991), or by microirradiation of kinetochores with a laser (McNeill and Berns, 1981). PSCS has been documented in two *Drosophila* meiotic mutants, *orientation disruptor* (*ord*) (Goldstein, 1980; Lin and Church, 1982) and *mei-S332* (Davis, 1971; Kerrebrock et al., 1992). Finally, several cytological features of *zw10* mutations, including aneuploidy and lagging chromatids at anaphase, have been noted both in *Drosophila* mutant for the gene *rough deal* (*rod*) (Karess and Glover, 1989) and in cell cultures derived from patients with the human genetic disorder Roberts Syndrome (Jabs et al., 1991).

A puzzling phenotypic consequence of mutations in *zw10* arises from the survival of a small number of "escaper" adults of both sexes that are either hemizygous or homozygous for all known *zw10* mutations. Both male and female escapers are sterile and exhibit a variety of cuticular defects (Shannon et al., 1972). Although the sterility of *zw10* escaper females can be explained by embryonic mitotic defects we have observed in their progeny, the fact that mutant hemizygous males contain immotile sperm (Shannon et al., 1972; our own unpublished observations) is more difficult to understand. Examination of the "onion stage" of spermatogenesis in mutant testes shows the presence of variable-sized spermatid nuclei, indicating that chromosomal nondisjunction or chromosome loss has occurred in the male germline. However, this alone does not account for sperm immotility: even sperm that contain only the tiny fourth chromosome are motile and capable of fertilization (Lindsley and Grell, 1969). The *zw10* product might therefore play an additional role in spermatogenesis or sperm function that is independent of chromosome segregation.

zw10 Protein Is Dynamically Localized in Mitotic Structures

Embryonic *zw10* protein undergoes cell-cycle dependent redistribution to different components of the mitotic apparatus. At the prophase–prometaphase transition, *zw10* protein becomes localized in the nuclear domain, and becomes associated with, or forms, a filamentous structure which persists through metaphase. A very rapid transition to a region at or near kinetochores is seen coincident with anaphase onset. At telophase, the *zw10* protein is excluded from the reforming nuclear domain and becomes dispersed in the cytoplasm. The dynamic nature of *zw10* distribution through these cell cycles is most likely because of intracellular movement of the same protein pool, rather than to reflect new protein synthesis, given the rapidity of embryonic nuclear divisions (Foe and Alberts, 1983).

The nature of the structures recognized by anti-*zw10* antibodies at metaphase and anaphase is uncertain. It is possible that the *zw10* protein filaments form an independent structure not directly associated with MTs. Alternatively, some manner of *zw10* association with spindle MTs would seem possible. It is clear that the *zw10* antigen could not be associated

with all MTs within the spindle, but is instead generally confined to a narrower region than the wide barrel-shaped spindle (Fig. 7 *C*). Thus, *zw10* protein may be specifically associated with the KMTs, in accordance with its movement to the kinetochore region at anaphase onset. Moreover, although *zw10* protein colocalizes with the leading edges of the chromosomes during anaphase at the resolution of light microscopy, we have no evidence that this site corresponds to the kinetochore per se. The resolution of these issues awaits further ultrastructural and biochemical studies.

The *zw10* protein does not appear to correspond to any of the large number of proteins already known to inhabit the mitotic spindle or the kinetochore/centromere. Such proteins have been identified by several protocols: as microtubule-associated proteins (MAPs) based on their copurification with MTs (reviewed by Olmstead, 1986; Kellogg et al., 1989), on the basis of antisera obtained by immunization against nuclei (Frasch et al., 1986) or mitotic chromosome scaffolds (Compton et al., 1991), or as polypeptides recognized by antisera from various patients with autoimmune disease (CREST sera; Moroi et al., 1980). Recently, it has also been observed that cytoplasmic dynein is associated with kinetochores and the spindle (Pfarr et al., 1990; Steuer et al., 1990; Wordeman et al., 1991). To our knowledge, none of these or other components show the same pattern of cell cycle-specific localization as *zw10* (see Brinkley, 1990; Pluta et al., 1990; Pankov et al., 1990; Earnshaw and Cooke, 1991).

The structure assumed by the *zw10* antigen at metaphase is strongly evocative of the location of an antigen called *spoke* (Paddy and Chelsky, 1991). Anti-*spoke* antibodies stain KMTs, revealing a filamentous structure with a regular helical substructure, similar to that seen in Fig. 6, *b* and *e* and Fig. 7, *A–C*. However, we do not believe that *zw10* represents the *Drosophila* homolog of *spoke*: unlike *spoke*, the metaphase structures identified by anti-*zw10* antibodies extend through the chromosomal mass. Furthermore, *spoke* is not redistributed onto kinetochores at anaphase, and instead remains associated with KMTs (Paddy and Chelsky, 1991). It nonetheless remains possible that the *zw10* metaphase structure is formed in association with a putative *Drosophila spoke* polypeptide.

The Role of zw10 in Mitotic Chromosome Segregation

Although the cytological evidence clearly shows that the *zw10* product is required to ensure the accuracy of mitotic chromosome segregation, several unresolved issues preclude precise determination of its molecular function. Perhaps most importantly, we do not yet understand the significance of the high levels of PSCS observed in colchicine-treated *zw10* neuroblasts. It is unclear whether this phenomenon monitors some indirect but nonetheless differential response of *zw10* and wild-type brain cells to colchicine, or instead indicates differences in some inherent property of the centromeric attachment between sister chromatids. In addition, because *zw10* mutations do not result in cell cycle arrest, *zw10* activity cannot be unambiguously ascribed to a particular phase of the cell cycle. In spite of these gaps in our knowledge, the available cytological and immunocytochemical results nonetheless provides some clues to the possible roles played by the *zw10* protein.

zw10 protein in the structure seen during metaphase that is roughly coincident with the spindle could be imagined to function in any of several ways. This protein could be of importance for spindle organization, for chromosome attachment or anchorage to the spindle, for ensuring the bipolar connection of sister kinetochores to opposite spindle poles, or for chromosomal movement during congression to the metaphase plate. However, preliminary three-dimensional observations in *zw10* mutant brains and in embryos produced by homozygous mutant germline clones show no obvious defects in the structures of the metaphase spindle or of the metaphase plate (our own unpublished results). Of course, we cannot exclude the possibilities that subtle metaphase defects occur, or that *zw10* activity during metaphase is required for subsequent anaphase movements. In addition, it should be remembered that one phenotypic effect of *zw10* mutations, that of PSCS, presumably occurs during a metaphase-like state induced by colchicine (González et al., 1991).

We believe that hypotheses predicting an activity of *zw10* protein at anaphase onset (rather than earlier at metaphase) are more compatible with the apparent normality of metaphase in mutants and with the extremely rapid transition between metaphase and anaphase locations of the *zw10* antigen. The nature of the signals governing entry into anaphase remain quite mysterious (Murray et al., 1989), and little is understood of the crucial process that breaks the centromeric connection between sister chromatids at the beginning of anaphase (Murray and Szostak, 1985). We can thus only guess at the manner by which the movement of *zw10* to the kinetochore region at anaphase onset could influence the accuracy of sister chromatid disjunction.

zw10 could be imagined to be a partially redundant component of a system positively required to activate sister chromatid separation or chromatid movement to the poles. Alternatively, *zw10* protein could act as a feedback control rendering certain events at anaphase onset dependent upon the successful completion of earlier events. For example, *zw10* might help ensure that anaphase will not begin if the spindle is not intact or if one or more chromosomes have not yet become properly aligned at the metaphase plate. It has been suggested that kinetochores unattached to the spindle may generate signals blocking anaphase onset (Zirkle, 1970; Ault and Nicklas, 1989; Rieder and Alexander, 1989; Bernat et al., 1991). Recently, "checkpoint" genes that apparently fulfill such a role have been found in yeast by Li and Murray (1991) and by Hoyt et al. (1991). Because we observe no obvious changes in cell cycle progression in *zw10* mutants (Table II), delays of anaphase onset caused by *zw10*$^+$ activity would have to be quite short. In a different scenario, *zw10*$^+$ might render sister chromatid separation dependent upon M phase promoting factor (MPF) inactivation, which is normally a precondition for most anaphase events (Murray et al., 1989). Loss of such *zw10*$^+$-mediated feedback inhibition could potentially explain the PSCS phenomenon observed in colchicine-treated mutant neuroblasts that retain high levels of MPF activity (Whitfield et al., 1990).

The unexpected distribution of the *zw10* protein as a function of the cell cycle remains difficult to interpret in terms of molecular activities that explain the observed phenotypes. We nonetheless believe that these initial results are sufficiently intriguing that future studies of the *zw10* protein and phenotype will provide unique insights into the function of the spindle and of the centromere/kinetochore.

We thank Maurizio Gatti, David Glover, and the members of their respective laboratories for their generosity, advice and assistance. We are indebted to Burke Judd and Abe Schalet for fly stocks, David Glover for anti-centrosome antibodies, Janis Werner for embryo microinjection, Gerry Chu for providing Northern blot strips, Ingrid Monteleone for supplying fly media, Diane LaPoint and Deborah Whiting for help with antibody production, and James Slattery, Carol Bayles, and Cathy Anderson for assistance with the confocal microscope at Cornell.

This work was supported by National Institutes of Health (NIH) grant GM13935 and an NIH Fogarty Center Senior International Fellowship to M. L. Goldberg. B. C. Williams was supported by NIH training grant GM07617 to the Field of Genetics and Development at Cornell University.

Received for publication 3 February 1992 and in revised form 13 May 1992.

References

Ault, J. G., and R. B. Nicklas. 1989. Tension, microtubule rearrangements, and the proper distribution of chromosomes in mitosis. *Chromosoma (Berl.).* 98:33–39.

Bernat, R. L., M. R. Delannoy, N. F. Rothfield, and W. C. Earnshaw. 1991. Disruption of centromere assembly during interphase inhibits kinetochore morphogenesis and function in mitosis. *Cell.* 66:1229–1238.

Bond, B. J., and N. Davidson. 1986. The *Drosophila* melanogaster actin 5C gene uses two transcription initiation sites and three polyadenylation sites to express multiple mRNA species. *Mol. Cell. Biol.* 6:2080–2088.

Brinkley, B. R. 1990. Centromeres and kinetochores: integrated domains on eukaryotic chromosomes. *Curr. Opin. Cell Biol.* 2:446–452.

Brinkley, B. R., A. Tousson, and M. M. Valdivia. 1985. The kinetochore of mammalian chromosomes: structure and function in normal mitosis and aneuploidy. *In* Aneuploidy, Etiology and Mechanisms. V. L. Dellarco, P. E. Voytek, and A. Hollaender, editors. Plenum Publishing Corp., New York. 243–267.

Brown, N. H., and F. C. Kafatos. 1988. Functional cDNA libraries from *Drosophila* embryos. *J. Mol. Biol.* 203:425–437.

Cavener, D. R., and S. C. Ray. 1991. Eukaryotic start and stop translation sites. *Nucleic Acids Res.* 19:3185–3192.

Compton, D. A., T. J. Yen, and D. W. Cleveland. 1991. Identification of novel centromere/kinetochore-associated proteins using monoclonal antibodies generated against human mitotic chromosome scaffolds. *J. Cell Biol.* 112: 1083–1097.

Davis, B. K. 1971. Genetic analysis of a meiotic mutant resulting in precocious sister-centromere separation in *Drosophila melanogaster. Mol. & Gen. Genet.* 113:251–272.

Devereux, J., P. Haeberli, and O. Smithies. 1984. A comprehensive set of sequence analysis programs for the VAX. *Nucleic Acids Res.* 12:387–395.

Dieckmann, C. L., and A. Tzagoloff. 1985. Assembly of the mitochondrial membrane system: *CPB6*, a yeast nuclear gene necessary for synthesis of cytochrome b. *J. Biol. Chem.* 260:1513–1520.

Dombrádi, V., J. M. Axton, D. M. Glover, and P. T. W. Cohen. 1989. Cloning and chromosomal localization of *Drosophila* cDNA encoding the catalytic subunit of protein phosphatase 1α. *Eur. J. Biochem.* 183:603–610.

Driver, A., S. F. Lacey, T. E. Cullingford, A. Mitchelson, and K. O'Hare. 1989. Structural analysis of Doc transposable elements associated with mutations at the *white* and *suppressor of forked* loci in *Drosophila melanogaster. Mol. & Gen. Genet.* 220:49–52.

Earnshaw, W. C., and C. A. Cooke. 1991. Analysis of the distribution of the INCENPs throughout mitosis reveals the existence of a pathway of structural changes in the chromosomes during metaphase and early events in cleavage furrow formation. *J. Cell Sci.* 98:443–461.

Feinberg, A. P., and B. Vogelstein. 1983. A technique for radiolabeling DNA restriction endonuclease fragments to high specific activity. *Anal. Biochem.* 132:6–13.

Foe, V. E. 1989. Mitotic domains reveal early commitment of cells in *Drosophila* embryos. *Development (Camb).* 107:1–22.

Foe, V. E., and B. M. Alberts. 1983. Studies of nuclear and cytoplasmic behavior during the five mitotic cycles that precede gastrulation in *Drosophila* embryogenesis. *J. Cell Sci.* 61:31–70.

Frasch, M., D. M. Glover, and H. Saumweber. 1986. Nuclear antigens follow different pathways into daughter nuclei during mitosis in early *Drosophila* embryos. *J. Cell Sci.* 82:155–172.

Gatti, M., and B. S. Baker. 1989. Genes controlling essential cell-cycle functions in *Drosophila melanogaster. Genes & Dev.* 3:438–453.

Gatti, M., and M. L. Goldberg. 1991. Mutations affecting cell division in *Drosophila. Methods Cell Biol.* 35:543–586.

Gatti, M., C. Tanzarella, and G. Olivieri. 1974. Analysis of the chromosome aberrations induced by X-rays in somatic cells of *Drosophila melanogaster. Genetics.* 77:701–719.

Goldberg, M. L., J. Y. Sheen, W. J. Gehring, and M. M. Green. 1983. Unequal crossing-over associated with asymmetrical synapsis between nomadic elements in the *Drosophila melanogaster* genome. *Proc. Natl. Acad. Sci. USA.* 80:5017–5021.

Goldstein, L. 1980. Mechanisms of chromosome orientation revealed by two meiotic mutants in *Drosophila melanogaster. Chromosoma (Berl.).* 78:79–111.

González, C., J. Casal, and P. Ripoll. 1988. Functional monopolar spindles caused by mutation in *mgr*, a cell division gene of *Drosophila melanogaster. J. Cell Sci.* 89:39–47.

González, C., J. C. Jimenez, P. Ripoll, and C. E. Sunkel. 1991. The spindle is required for the process of sister chromatid separation in *Drosophila* neuroblasts. *Exp. Cell Res.* 192:10–15.

Gunaratne, P. H., A. Mansukhani, S. E. Lipari, H.-C. Liou, D. W. Martindale, and M. L. Goldberg. 1986. Molecular cloning, germline transformation, and transcriptional analysis of the *zeste* locus of *Drosophila melanogaster. Proc. Natl. Acad. Sci. USA.* 83:701–705.

Guo, L.-H., P. P. Stepien, J. Y. Tso, R. Brousseau, S. Narang, D. Y. Thomas, and R. Wu. 1984. Synthesis of human insulin gene. VIII. Construction of expression vector for fused proinsulin production in *Escherichia coli. Gene (Amst.).* 29:251–254.

Henikoff, S. 1984. Unidirectional digestion with exonuclease III creates targeted breakpoints for DNA sequencing. *Gene (Amst.).* 28:351–359.

Hiraoka, Y., D. A. Agard, and J. W. Sedat. 1990. Temporal and spatial coordination of chromosome movement, spindle formation, and nuclear envelope breakdown during prometaphase in *Drosophila melanogaster* embryos. *J. Cell Biol.* 111:2815–2828.

Hoyt, M. A., L. Totis, and B. T. Roberts. 1991. *S. cerevisiae* genes required for cell cycle arrest in response to loss of microtubule function. *Cell.* 66:507–517.

Hsu, T., and K. Satya-Prakash. 1985. Aneuploidy induction by mitotic arrestants in animal cell systems. *In* Aneuploidy, Etiology and Mechanisms. V. L. Dellarco, P. E. Voytek, and A. Hollaender, editors. Plenum Publishing Corp., New York. 279–290.

Jabs, E. W., C. M. Tuck-Miller, R. Cusano, and J. B. Rattner. 1991. Studies of mitotic and centromeric abnormalities in Roberts syndrome: implications for a defect in the mitotic mechanism. *Chromosoma (Berl.).* 100:251–261.

Judd, B. H., M. W. Shen, and T. C. Kaufman. 1972. The anatomy and function of a segment of the X chromosome of *Drosophila melanogaster. Genetics.* 71:139–156.

Karess, R. E., and D. M. Glover. 1989. *rough deal*: a gene required for proper mitotic segregation in *Drosophila. J. Cell Biol.* 109:2951–2961.

Karr, T. L., and B. M. Alberts. 1986. Organization of the cytoskeleton in early *Drosophila* embryos. *J. Cell Biol.* 102:1494–1509.

Kellogg, D. R., C. M. Field, and B. M. Alberts. 1989. Identification of microtubule-associated proteins in the centrosome, spindle, and kinetochore of the early *Drosophila* embryo. *J. Cell Biol.* 109:2977–2991.

Kerrebrock, A. W., W. Y. Miyazaki, D. Birnby, and T. L. Orr-Weaver. 1992. The *Drosophila mei-S332* gene promotes sister-chromatid cohesion in meiosis following kinetochore differentiation. *Genetics.* 130:827–841.

Kidd, S., T. J. Lockett, and M. W. Young. 1983. The *Notch* locus of *Drosophila melanogaster. Cell.* 34:421–433.

Klemenz, R., U. Weber, and W. J. Gehring. 1987. The *white* gene as a marker in a new P-element vector for gene transfer in *Drosophila. Nucleic Acids Res.* 13:3947–3959.

Li, R., and A. W. Murray. 1991. Feedback control of mitosis in budding yeast. *Cell.* 66:519–531.

Lin, H.-P. P., and K. Church. 1982. Meiosis in *Drosophila melanogaster.* III. The effect of *orientation disruptor (ord)* on gonial mitotic and meiotic divisions in males. *Genetics.* 102:751–770.

Lindsley, D. L., and E. H. Grell. 1969. Spermiogenesis without chromosomes in *Drosophila melanogaster. Genetics.* 61(Suppl.):69–78.

Lindsley, D. L., and G. Zimm. 1986. The genome of *Drosophila melanogaster.* Part 2: lethals, maps. *Dros. Inf. Serv.* 64:1–158.

Lindsley, D. L., and G. Zimm. 1987. The genome of *Drosophila melanogaster.* Part 3: rearrangements. *Dros. Inf. Serv.* 65:1–224.

Lindsley, D. L., and G. Zimm. 1990. The genome of *Drosophila melanogaster.* Part 4: genes L–Z, balancers, transposable elements. *Dros. Inf. Serv.* 68:1–382.

Mansukhani, A., P. H. Gunaratne, P. W. Sherwood, B. J. Sneath, and M. L. Goldberg. 1988*a*. Nucleotide sequence and structural analysis of the *zeste* locus of *Drosophila melanogaster. Mol. & Gen. Genet.* 211:121–128.

Mansukhani, A., A. Crickmore, P. W. Sherwood, and M. L. Goldberg. 1988*b*. DNA-binding properties of the *Drosophila melanogaster zeste* gene product. *Mol. Cell. Biol.* 8:615–623.

McNeill, P. A., and M. W. Berns. 1981. Chromosome behavior after laser microirradiation of a single kinetochore in mitotic PtK2 cells. *J. Cell Biol.* 88:543–553.

Moroi, Y., M. J. Peebles, J. Fritzler, J. Steigerwald, and E. M. Tan. 1980. Autoantibody to centromere (kinetochore) in scleroderma sera. *Proc. Natl. Acad. Sci. USA.* 77:1627–1631.

Murray, A. W., and J. W. Szostak. 1985. Chromosome segregation in mitosis and meiosis. *Ann. Rev. Cell Biol.* 1:289–315.

Murray, A. W., M. J. Solomon, and M. W. Kirschner. 1989. The role of cyclin synthesis and degradation in the control of maturation promoting factor activity. *Nature (Lond.).* 339:280–286.

Olmsted, J. B. 1986. Microtubule-associated proteins. *Ann. Rev. Cell Biol.*

2:421–457.
Paddy, M. R., and D. Chelsky. 1991. Spoke: a 120-kD protein associated with a novel filamentous structure on or near kinetochore microtubules in the mitotic spindle. *J. Cell Biol.* 113:161–171.
Pankov, R., M. Lemieux, and R. Hancock. 1990. An antigen located in the kinetochore region in metaphase and on polar microtubule ends in the midbody region in anaphase, characterized using a monoclonal antibody. *Chromosoma (Berl.).* 99:95–101.
Perrimon, N., L. Engstrom, and A. P. Mahowald. 1989. Zygotic lethals with specific maternal effect phenotypes in *Drosophila melanogaster*. I. Loci on the X Chromosome. *Genetics.* 121:333–352.
Pfarr, C. M., M. Coue, P. M. Grissom, T. S. Hays, M. E. Porter, and J. R. McIntosh. 1990. Cytoplasmic dynein is localized to kinetochores during mitosis. *Nature (Lond.).* 345:263–265.
Pluta, A. F., C. A. Cooke, and W. C. Earnshaw. 1990. Structure of the human centromere at metaphase. *Trends Biol. Sci.* 15:181–185.
Rieder, C. L., and S. P. Alexander. 1989. The attachment of chromosomes to the mitotic spindle and the production of aneuploidy in newt lung cells. *In* Mechanisms of Chromosome Distribution and Aneuploidy. M. A. Resnick and B. K. Vig, editors. Alan R. Liss Inc., New York. 185–194.
Robertson, H. M., C. R. Preston, R. W. Phillis, D. Johnson-Schlitz, W. K. Benz, and W. R. Engels. 1988. A stable genomic source of P element transposase in *Drosophila melanogaster*. *Genetics.* 118:461–470.
Sambrook, J., E. F. Fritsch, and T. Maniatis. 1989. Molecular Cloning: A Laboratory Manual. Second Edition. Cold Spring Harbor Laboratory Press, Cold Spring Harbor, New York. Volumes 1–3.
Sanger, F., S. Nicklen, and I. R. Coulson. 1977. DNA sequencing with chain-terminating inhibitors. *Proc. Natl. Acad. Sci. USA.* 74:5463–5467.
Schalet, A. 1986. The distribution of and complementation relationships between spontaneous X-linked recessive lethal mutations recovered from crossing long-term laboratory stocks of *Drosophila melanogaster*. *Mutat. Res.* 163:113–144.
Shalloway, D., and S. Shenoy. 1991. Oncoprotein kinases in mitosis. *Adv. Cancer Res.* 57:185–225.
Shannon, M. P., T. C. Kaufman, M. W. Shen, and B. H. Judd. 1972. Lethality patterns and morphology of selected lethal and semi-lethal mutations in the *zeste-white* region of *Drosophila melanogaster*. *Genetics.* 72:615–638.
Smith, D. A., B. S. Baker, and M. Gatti. 1985. Mutations in genes controlling essential mitotic functions in *Drosophila melanogaster*. *Genetics.* 110: 647–670.
Stafstrom, J. P., and L. A. Staehelin. 1984. Dynamics of the nuclear envelope and of nuclear pore complexes during mitosis in the *Drosophila* embryo. *Eur. J. Cell Biol.* 34:179–189.
Steuer, E. R., L. Wordeman, T. A. Schroer, and M. P. Sheetz. 1990. Localization of cytoplasmic dynein to mitotic spindles and kinetochores. *Nature (Lond.).* 345:266–268.
Xiao, H., and J. T. Lis. 1989. Heat shock and developmental regulation of the *Drosophila melanogaster* hsp83 gene. *Mol. Cell. Biol.* 9:1746–1753.
Warn, R. M., and A. Warn. 1986. Microtubule arrays present during the syncytial and cellular blastoderm stages of the early *Drosophila* embryo. *Exp. Cell Res.* 163:201–210.
Whitfield, W. G. F., C. González, G. Maldonado-Codina, and D. M. Glover. 1990. The A and B type cyclins are accumulated and destroyed in temporally distinct events that define separable phases of the G2/M transition. *EMBO (Eur. Mol. Biol. Organ.) J.* 9:2563–2572.
Wordeman, L., E. R. Steuer, M. P. Sheetz, and T. Mitchison. 1991. Chemical subdomains within the kinetochore domain of isolated CHO mitotic chromosomes. *J. Cell Biol.* 114:285–294.
Zirkle, R. E. 1970. Ultraviolet-microbeam irradiation of newt-cell cytoplasm: spindle destruction, false anaphase, and delay of true anaphase. *Radiat. Res.* 41:516–537.